TOWARDS DEVELOPMENT OF SMART NANOSENSOR SYSTEM TO DETECT OF HYPOGLYCEMIA FROM BREATH

A Thesis

Submitted to the Faculty

of

Purdue University

by

Sanskar S. Thakur

In Partial Fulfillment of the

Requirements for the Degree

of

Master of Science in Mechanical Engineering

May 2020

Purdue University

Indianapolis, Indiana

THE PURDUE UNIVERSITY GRADUATE SCHOOL
STATEMENT OF THESIS APPROVAL

Dr. Mangilal Agarwal, Chair

Department of Mechanical and Energy Engineering

Dr. Andres Tovar

Department of Mechanical and Energy Engineering

Dr. Sohel Anwar

Department of Mechanical and Energy Engineering

Approved by:

Dr. Sohel Anwar

Chair of the Graduate Program

Dedicated to my Family and friends...

ACKNOWLEDGMENTS

I wish to express my gratitude towards my advisor and mentor Dr. Mangilal Agarwal for his administration, assistance, and liberty. He has inspired me to be innovative and has helped me explore my interest in research. I was able to move the research forward and complete my thesis under his supervision. I am also thankful to Dr. Tovar and Dr. Anwar for their valuable feedback and comments on my research, Dr. Ali Daneshkhah for his assistance and support in design and development of experiments, Dr. Amanda Siegel for her lessons on chemistry and technical writing, Dr. Nojan Alihamad for his support in FESEM, and other colleagues Mark Wollam and Paula Angarita for their assistance in the lab.

I am grateful to my parents for their endless support, love, and motivation to pursue my dreams. I would like to thank my aunt Dr. Ambuja Salgaonkar and Dr. Jayant Kirtane for their mentorship, and my roommates Ajinkya Gulhane and Hardik Peshawerya for emotional support away from home.

I would also like to acknowledge the National Science Foundation (NSF) to support this project under grant no. 1502310. Integrated Nanosystems Development Institute (INDI) is also acknowledged to provide an instrument used for the successful completion of this project..

TABLE OF CONTENTS

Page

LIST OF TABLES

LIST OF FIGURES

Figure Page

SYMBOLS

m	meter
μm	micrometer
mm	millimeter
nm	nanometer
C	Celsius
Ω	ohm
$K\Omega$	killo-ohm
s	seconds
rpm	rotations per minute
cc	cubic centimeter
RH	relative humidity
R_{t}	electron tunneling resistance
L	average separation gap between nanoparticles
β	electron tunneling decay constant
E_{A}	activation barrier energy
k	Boltzmann constant
T	temperature
V	volts
mV	millivolts
kV	kilovolts
ΔR	change in sensor resistance
R_0	initial sensor resistance

ABBREVIATIONS

T1D	type 1 diabetes
BG	blood glucose
CGMs	continuos glucose monitors
VOCs	volatile organic compounds
CNTs	Carbon Nanotubes
AI	artificial intelligence
eNose	electronic nose
IDEs	interdigitated electrodes
FESEM	field emission scanning electron microscope
UV/VIS	ultra-violet visivble spectroscopy
PVDF-HFP	poly(vinylidene fluoride -hexafluoropropylene)
PVDF-HFP-CB	poly(vinylidene fluoride -hexafluoropropylene)-carbon black
EGNP	ether functionalized gold nanoparticle
PEI	polyetherimide
DADs	diabetes alert dogs
OGTT	oral glucose tolerance test
MS	mass spectrometry
MRI	magnetic resonance spectroscopy
NMR	nuclear magnetic resonance
GC	gas chromatography
GC-FID	gas chromatography flame ionization detector
PTR-MS	proton transfer reaction mass spectrometry
GC-MS	gas chromatography mass spectrometry
m/z	ion mass to ion charge ratio
SPME	solid-phase microextraction

ANN	artificial neural network
ppm	parts per million
ppb	parts per billion
SAWS	surface acoustic wave sensor
f-GNPs	functionalized goldnanoparticles
CPCs	conducting polymer composites
MWCNTs	multi-walled carbon nanotubes
QCM	quartz crystal microbalance
MOS	metal oxide semiconductor
SWCNTs	single-walled carbon nanotubes
ICPs	intrinsically conducting polymers
LB	Langmuir-Blogdett
PWM	pulse-width modulation or pulse-width modulated
BLE	bluetooth low energy
PCA	principle component analysis
LDA	linear discriminant analysis
IS	integrated signal
RT	retention time
AUC	area under the curve
ROC	receiver operating characteristic
NMP	1-Methyl- 2-pyrrolidinone
DEC	diethylene carbonate
MFCs	mass flow controllers
SCCM	standard cubic centimeters per minute
Bluno	Arduino Bluno nano with on-board bluetooth low energy
IPA	isopropanol
PCB	printed circuit board
MUX	multiplexer/demultiplexer 74HC4052D
SPR	surface plasmon resonance

ABSTRACT

Thakur, Sanskar S. M.S.M.E., Purdue University, May 2020. Towards Development of Smart Nanosensor System to Detect of Hypoglycemia from Breath. Major Professor: Mangilal Agarwal.

The link between volatile organic compounds (VOCs) from breath and various diseases and specific conditions has been identified since long by the researchers. Canine studies and breath sample analysis on Gas chromatography/ Mass Spectroscopy has proven that there are VOCs in the breath that can detect and potentially predict hypoglycemia. This project aims at developing a smart nanosensor system to detect hypoglycemia from human breath. The sensor system comprises of 1-Mercapto-(triethylene glycol) methyl ether functionalized goldnanoparticle (EGNPs) sensors coated with polyetherimide (PEI) and poly(vinylidene fluoride -hexafluoropropylene) (PVDF-HFP) and polymer composite sensor made from PVDF-HFP-Carbon Black (PVDF-HFP/CB), an interface circuit that performs signal conditioning and amplification, and a microcontroller with Bluetooth Low Energy (BLE) to control the interface circuit and communicate with an external personal digital assistant. The sensors were fabricated and tested with 5 VOCs in dry air and simulated breath (mixture of air, small portion of acetone, ethanol at high humidity) to investigate sensitivity and selectivity. The name of the VOCs is not disclosed herein but these VOCs have been identified in breath and are identified as potential biomarkers for other diseases as well.

The sensor hydrophobicity has been studied using contact angle measurement. The GNPs size was verified using Ultra-Violent-Visible (UV-VIS) Spectroscopy. Field Emission Scanning Electron Microscope (FESEM) image is used to show GNPs embedded in the polymer film. The sensors sensitivity increases by more than 400% in an environment with relative humidity (RH) of 93% and the sensors show selectivity

towards VOCs of interest. The interface circuit was designed on Eagle PCB and was fabricated using a two-layer PCB. The fabricated interface circuit was simulated with variable resistance and was verified with experiments. The system is also tested at different power source voltages and it was found that the system performance is optimum at more than 5 volts. The sensor fabrication, testing methods, and results are presented and discussed along with interface circuit design, fabrication, and characterization.

1. INTRODUCTION

1.1 Objective

Hypoglycemia (low blood sugar) is a transient condition that can leads to complications such as dizziness, fainting, to fatal nerve damage, coma and in worst cases death [1]. It is very important for people with diabetes who are susceptible to hypoglycemia (all people with type 1 diabetes(T1D) and some with type 2 diabetes) to monitor and maintain their blood glucose (BG) level to avoid a hypoglycemic attack. Most traditional glucose monitoring methods for T1D require glucose measurement from blood samples (glucometers) or interstitial fluids (continuous glucose monitors or CGMs). These methods are invasive, can be mentally and physically stressful for patients. In addition, CGMs have 20 minutes lag to actual blood glucose values [2]. The current thesis describes research towards a novel system for monitoring blood glucose through chemiresistive sensors specifically tuned to detect volatile organic compounds (VOCs) that are produced during hypoglycemia. The research described includes chemical and statistical analysis for identifying VOCs of interest from breath samples acquired from children and adults with T1D. Here, breath samples were analyzed by gas chromatography-mass spectrometry. The research continues with a description of chemiresistive sensors that are specific to the VOCs of hypoglycemia. Functionalized gold nanoparticles and conductive polymer composites have been seen to have better control over selectivity, sensitivity, lower operating temperatures and response time over other chemiresistive materials like carbon nanotubes (CNTs) and graphene [3] [4] [5]. Finally, the research includes incorporation of these sensors into a smart and connected system comprised of 1) an array of gas sensors specifically designed to detect VOCs of hypoglycemia, 2) an interface circuit that performs the signal conditioning and amplification, and 3) signal processing unit that uses artifi-

cial intelligence (AI) to perform data analysis and extract features. In this way, the research is a significant advance over nonspecific collections of gas arrays that process VOCs and which are commonly known as electronic nose (eNose) systems. The research builds on other work at IUPUI towards identifying and validating biomarkers for hypoglycemia, and preliminary sensor elements fabricated and newly incorporated into the current smart and connected system [6]. In this way, the research presents significant steps toward a portable sensor system to detect and potentially predict hypoglycemia.

1.1.1 Research Approach

The construction of the thesis is elaborated here. The objective and outline are described in Chapter 1. A literature review is presented in chapter 2, where the importance of noninvasive biomarker detection is explained. It also briefs about research done in the field of biomarker discovery and detection, technologies and analytical tools used to detect VOCs to compare and implement the best suitable technology. Chapter 3 explains the materials and methods that are used to fabricate sensors and the sensor interface circuit. This chapter will also describe the fabrication of interdigitated electrodes (IDEs), synthesis and fabrication of sensing material over IDEs, fabrication of sensors, as well as design and fabrication of an electrical interface circuit and packaging for the sensor system. Chapter 4 describes material characterization results that include contact angle measurement, Field Emission Scanning Electron Microscope (FESEM), Ultra-violet Visible Spectroscopy (UV/VIS), and profilometer measurement of fabricated films. The sensors fabricated using poly(vinylidene fluoride -hexafluoropropylene) (PVDF-HFP) composite with carbon black (PVDF-HFP-CB), 1-Mercapto-(triethylene glycol) methyl ether functionalized GNPs (EGNP) with polyetherimide (PEI) and a PVDF-HFP layer are tested with multiple VOCs and with simulated breath and the results are presented in Chapter 4. The characterization of the interface circuit and sensor integration results with interface circuit are is also

presented in chapter 4. Chapter 5 presents the conclusion made regarding sensor response towards VOCs and also describes future work related to the nanosensor system.

2. LITERATURE REVIEW

2.1 VOC Analysis for Noninvasive Disease Detection

T1D is an autoimmune disease that causes the body to fail to produce insulin. Insulin is a hormone that is required to carry glucose from the bloodstream into the cells. T1D develops when the body's immune system attacks pancreatic beta cells which are responsible for insulin production [7]. Around 1.25 million Americans have T1D and around 40,000 people are newly diagnosed with T1D every year in the United States [8]. Out of these 1.25 million, about 200,000 are less than 20 years old [9]. Patients with T1D need to control their glucose levels by using external insulin and measured food intake. Diabetes patients who take insulin are susceptible to hypoglycemic events or episodes due to excess insulin. Hypoglycemic events can occur at any time and can have no symptoms at the beginning which makes it more dangerous. According to the American Diabetes Association, ADA, an average number of episodes for an average patient is two per week, not including the lows without symptoms. Hypoglycemic episodes during the night have also been cited as a cause of death [1]. It is one of the most feared complications of T1D and can lead patients to have an inadequate intake of insulin [10]. Therefore, blood glucose levels are required to be monitored frequently to avoid critical situations. A clinical study involving 16,000 patients with T1D, conducted over two years, showed that 75% of children and youth (ages 7 to 21) were unable to maintain proper glycemic control [11].

Several studies have shown that dogs can detect hypoglycemia and alert the subject with or without training [12] [13] [14] [15] [16]. Diabetic alert dogs (DADs) have been implemented to alert patients and researchers have studied dog's ability to sniff other diseases such as cancer [13] . This method utilizes canine's ultrasensitive nose and ability to differentiate slight changes in breath, urine, sweat, or saliva composi-

tion. Dogs have up to 300 million olfactory receptors in their nose while humans have only about 5 million. Studies have shown improved well-being and fewer paramedic visits for patients with DADs [17] [18]. Though it is an effective way to alert patients with hypoglycemia, canines are expensive and require time-consuming/continuous training. Also, DADs may not perform their trained behavior even after detecting the odor due to external or behavioral factors.

Biomarkers are defined as "a substance, structure or process that can be measured in the body or its products and influence or predict the incidence of outcome or disease" [19] [20]. Biomarker discovery involves the measurement of macromolecules, cells, or other processes that can describe the biological abnormality of an organism [21]. There has been considerable research on the identification of breath biomarkers for various diseases like lung cancer [22] [23], breast cancer [24] [24], colon cancer [25], prostate cancer [25], Alzheimer's [26], Parkinson's [26] , hyperglycemia [27] , and diabetes [6] [27] [28] [29] [30] [31]. One breath study on the oral glucose tolerance test (OGTT) found a relation between breath biomarker and gestational diabetes but were unable to correlate it without the OGTT [32]. Clinical studies for hyperglycemia have found VOCs that can predict high blood sugar after calibration [27] [33]. A few research groups found a relation of acetone and isoprene with hypoglycemia as potential biomarkers but these volatiles have also been seen during exercise [30] [34] . All these studies indicate that it is possible to find a panel of VOC biomarkers to detect hypoglycemia. Researchers are currently searching for noninvasive methods for monitoring glucose from saliva, tears, and sweat [35]. One such recently developed method involves canines (DADs) trained to sniff hypoglycemia from saliva [36] [37], or breath samples [38]. This method does not involve monitoring blood glucose levels but relies on the detection of changes in volatiles (or VOCs). The disease or condition can alter the metabolism of the body which affects the VOC concentration in the blood, this blood interacts with alveolar air in the lungs and the VOCs are exhaled with the breath. Since VOCs are a result of changes in the metabolic process, VOC analysis can be used to predict a condition affecting the metabolic process before the

actual symptoms are seen. Researchers have studied the trend in VOCs during the progression of a disease to see if a disease can be predicted/detected in early stages.

To avoid the physical and mental stress caused due to invasive diagnosis techniques such as biopsy and blood sample testing which can result in false detection, researchers are looking for various non-invasive techniques to diagnose diseases including prostate cancer, ovarian cancer, lung cancer and even Alzheimer's. The primary sample matrices for such non-invasive techniques are body fluids like urine, saliva, and sweat and exhaled breath.

2.2 Analytical Tools for VOCs Detection

Exhaled breath can be used to evaluate the health of a subject in regard to a disease or specific conditions. Biological breath samples consist of ambient air mixed with gases produced endogenously including VOCs and CO_2, coupled with water and small amount of non-volatiles including cytokines [39]. Researchers have explored the metabolic processes linked to diabetes by microanalysis of breath samples using mass spectrometry (MS) [27], magnetic resonance spectroscopy (MRI) and nuclear magnetic resonance (NMR) [40]. Commonly used techniques for analyzing samples of breath to identify endogenous VOCs can be divided into three major groups:

1) Laser – absorption spectroscopic techniques

2) Mass spectrometric techniques

3) Electronic noses (eNoses)

2.2.1 Laser – Absorption Spectroscopic Techniques

Laser Spectroscopy uses a laser beam to inspect analytes in the gas phase inside a cell. The gas molecules absorb very specific wavelengths of electromagnetic radiation and can be detected by identifying unique fingerprints. The technique has a very high resolution and can detect ultra-low (10 ppb) concentrations of NO [41]. This technique has been used to detect aldehydes (biomarkers for lung cancer and breast

cancer) [42]. The low sensitivity, high noise and drift between two consecutive readings is major concern with this technique for breath analysis. Due to this reasons, the method is not preferred.

2.2.2 Mass Spectrometric Techniques

GC- flame ionization detector (GC-FID) is another commonly used method for organic compound detection but not identification. It has high sensitivity, linear response, and low noise. The organic compounds are burnt in FID to produce ions and electrons. The electric potential through these ions is used for quantification [43].

Ion Mobility Spectrometry, IMS, separates VOCs based on the mobility of ions through the purified gas in an electric field. Factors like drift length, temperature, drift gas type and atmospheric pressure can account for determining total travel time for ions. Proton transfer reaction- mass spectrometry (PTR-MS) is suited for on-line, multiple measurements. The analyte is ionized by PTR with primary ion H_3O^+ [44]. It does not require preprocessing and the compounds with high abundance do not interfere with target compound detection. Selected Ion Flow Tube MS, SIFT-MS, combines fast-flow tube technique to MS, giving real-time quantification for various VOCs [45] [46] [47]. Here the VOCs react with precursor ions inside the flow tube at a controlled rate and the ions are analyzed quantitatively by MS. It has been used to quantify isoprene in breath samples of 29 healthy volunteers over 6 months [48].

Gas chromatography-mass spectrometry (GC-MS) is the most common methods used for breath analysis of VOCs. GC-MS is a combination of two microanalytical techniques: gas chromatography allows the separation of various components of the sample in time while mass spectrometry allows identification of the components based on the fragmentation pattern induced by ionization following elution from the column. GC-MS not only separates the components in the sample and provides qualitative data based on the spectra, but also provides quantitative data for the same components [49]. Elevated pressure is required for separation of components in GC and greatly

reduced pressure is used in MS to separate the ion of various mass to charge ratios (m/z). It is the most commonly used technique to detect volatiles in healthcare, medical, forensics, food safety, environmental science, and many other industries. Solid-phase microextraction (SPME) is usually used to extract and preconcentrate VOCs prior to GC-MS analysis. SPME uses a fiber coated with an extracting phase (liquid or solid) that can bind different VOCs with varying affinity. After extraction, the fiber is then injected into the GC inlet where the volatiles thermally desorb and enter the chromatographic column to be separated, identified and quantified. Raw GC-MS data from biological samples needs to be deconvoluted and spectrally aligned as it contains overlapping peaks and noise.

A study on breath odor compounds for liver patients using GC-MS found that it is possible to discriminate patients with hepatic pathologies [50]. Another study on human breath using SPME- GC-MS found hydrocarbons, ethers, esters, ketones, aldehydes and alcohols in healthy human breath [51]. Breath analysis has also been used to detect lung cancer [52] [53]. It has been previously demonstrated that it is possible to detect and discriminate between lung, breast, colorectal, and prostate cancer from healthy via GC-MS analysis of breath [25]. It has also been used to analyze biomarkers for T1D, hyperglycemia, hypoglycemia [27] [54]. Siegel et al. have shown that GC-MS can be used to analyze breath samples and identify a hypoglycemic-specific signature which could differentiate between hypoglycemic and normal (euglycemic) samples with high accuracy [6].A study on mouse urine using GC-MS has also shown that the data can discriminate between metastatic and local models of breast cancer [55].

2.2.3 Electronic Noses (eNoses)

GC-MS has been a golden standard for VOC analysis, however, it is costly and time-consuming. GC-MS also requires trained personnel and is not suitable for the desired point of care application. An alternative to the GC-MS is the eNose, a small-

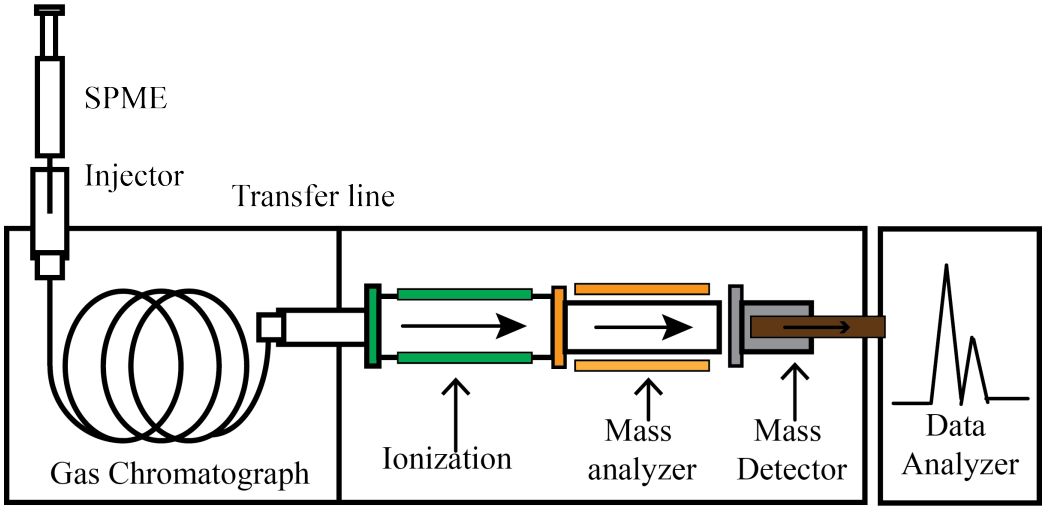

Figure 2.1. Schematics of Gas Chromatography Mass Spectroscopy instrument

portable devices that use a variety of gas sensing technologies to identify various gases from a mixture. An eNose can detect and discriminate VOC patterns from a complex gaseous mixture like biological breath samples. The basic eNose system has a multisensory array to detect the VOCs and generate a signal, transducer that converts sensor signal into readable value, software for recording the data, an artificial neural network (ANN) to perform pattern recognition and statistical analysis. eNose is ideal for noninvasive, real-time diagnosis due to its ability to characterize and discriminate between clinical samples based on VOCs [56] [57] [58] [59]. Researchers have shown its ability to detect cancer, malaria, asthma, and other diseases [60] [61] [62] [63] [64]. It is unique due to its ability to characterize and discriminate between clinical samples based on the sensors response to the VOCs [56] [57] [59] [58] using AI. The eNose is comprised of 1) an array of gas sensors to detect the different gas molecules, 2) an interface circuit that performs the signal conditioning and amplification on the sensory signal, and 3) signal processing unit that uses AI to perform data analysis and extract features. The eNoses can comprise of other components based on specifications and features like communication and interfacing. Most commonly used sensors in eNose systems are chemiresistors due to ease of

integration and signal conditioning. However, due to its bulky nature and black box approach, eNoses have limited application and need lot of samples to train the system to detect a specific signature as it is hard to detect specific biomarkers.

2.3 Gas Sensing Technologies

Gas sensing technologies that are commonly used to detect volatiles are discussed here. Brief introduction to the technology and its application in the volatile sensing are described.

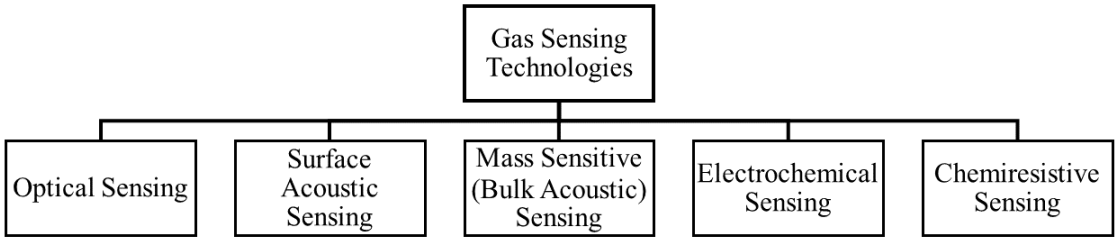

Figure 2.2. Types of Gas Sensing Technologies

2.3.1 Optical Sensing

Colorimetric sensors and infrared sensors both give optical results with fast response and high sensitivity and selectivity. Colorimetric sensors are composed of chemically sensitive dyes that respond to the analytes based on the reactivity of the VOCs. The compounds are detected based on a change in the color of dyes in the sensor array. Eaidkong et al. have successfully distinguished 18 VOCs (toluene, benzene, pentene and others) using a three polydiacetylene paper-based photodiode array of sensors [65]. Another research group reported a pre-oxidation technique to improve detection and identification of 20 indoor VOC pollutants including acetone, toluene,

p-xylene and isopropanol [66]. infrared or IR sensors, on the other hand, discriminate volatiles based on the absorption of a specific wavelength of light. Researchers have detected benzene, acetic acid, ethanol, toluene and dimethylamine using optical fiber sensors with sensing layer of polyvinyl pyrrolidone, PVP, at low concentrations (1 to 10 ppb) [67].

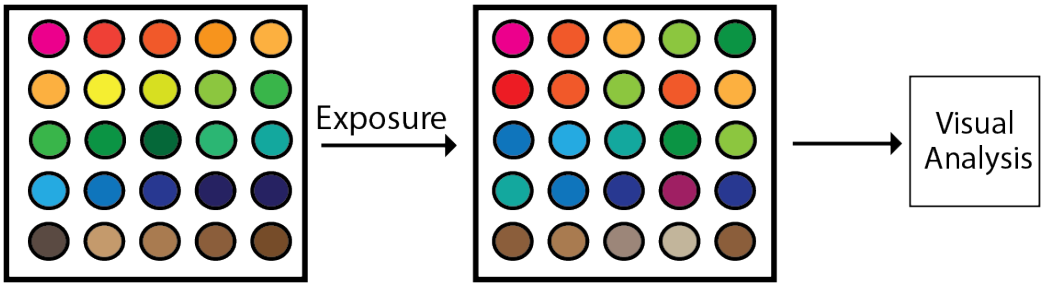

Figure 2.3. Colorimetric Sensor

2.3.2 Surface Acoustic Sensing

Acoustic sensors detect gas molecules based on a change in wave amplitude and velocity due to change in sensing film. These sensors have a low detection limit, fast response time and low fabrication cost. The selectivity and sensitivity of surface acoustic wave sensor (SAWS) depend on the nature of sensing film. Generally, a very thin and homogeneous layer of sensing material is desired for high signal to noise ratio and short response time. SAWS were introduced for chemical sensing application by Wohltjen and Dessy in 1979 [68]. Many researchers have used this technology for VOC detection in recent studies. Viespe and Grigoriu used this principle to detect low concentrations of methanol, ethanol, and toluene using a thin layer of SiO_2 /Si nanoparticles and multi-walled carbon nanotubes (MWCNTs) embedded on polymer layer [69] [70].

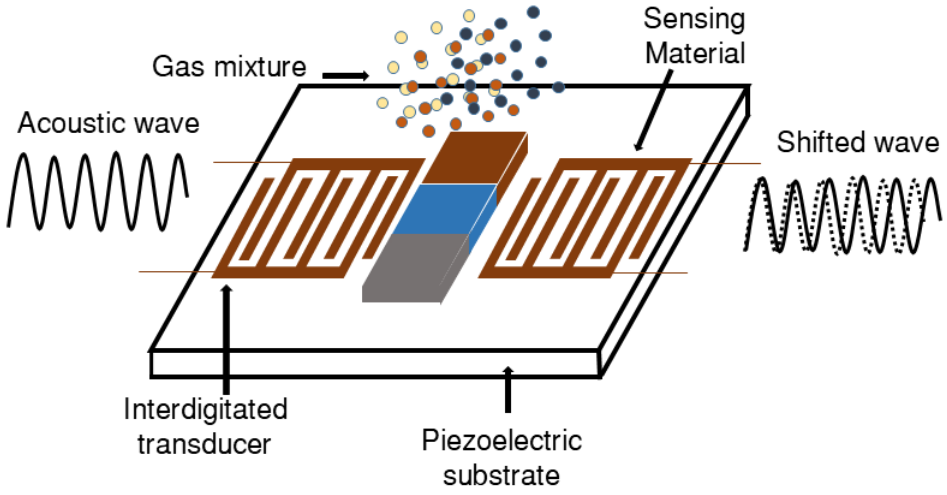

Figure 2.4. Surface Acoustic Sensing Principle

2.3.3 Mass Sensitive (Bulk Acoustic) Sensing

Mass sensitive sensors measure the change in mass occurring due to adsorption of gas molecules on the sensing surface. The majority of the mass sensors are based on piezoelectric bulk oscillators, but sometimes vibrating beams are also used for detection [71]. The commonly used oscillators are quartz crystal oscillators/microbalance (QCM), it has been used to detect p-xylene[73], toluene, ethanol, 1-octanol, acetic acid and acetone [72]. QCM sensors have shown good sensitivity towards aromatic compounds, alcohols, amines, and ketones [73] [74] [23].

2.3.4 Electrochemical Sensing

Electrochemical sensors are based on reduction/oxidation (redox) reactions proceeding at the electrodes. The electrolyte solution interacts with analyte VOCs. The reaction at the working electrode which is polarized based on the reference electrode generates a signal in the form of change in either current (amperometric sensors), voltage (potentiometric sensors) or admittance (conductometric sensors) [75] [76].

This type of sensors is used commercially to detect toxic compounds in the air [77]. These sensors are not preferred for breath analysis application as it needs electrolyte that can be hazardous if exposed to human breath.

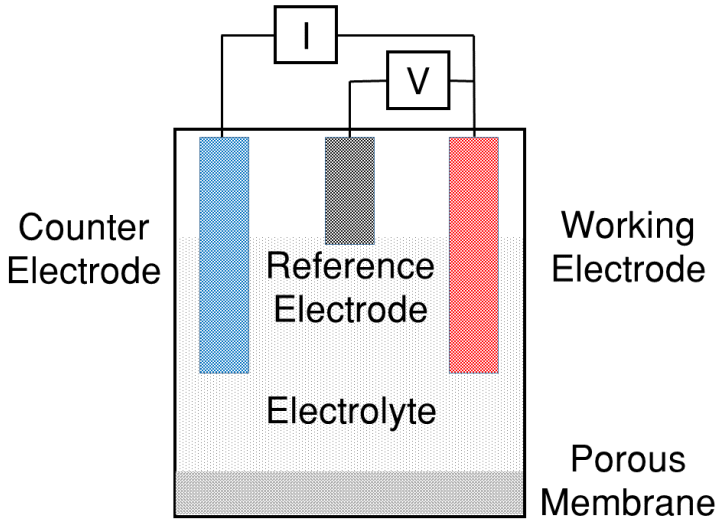

Figure 2.5. Electrochemical Sensing Principle

2.3.5 Chemiresistive Sensing

These sensors detect and quantify the concentration of different gases based on a change in the resistance of sensors due to the variation in the molecular structure of the sensing material. The molecular structure of the sensing element changes as the gas molecules are introduced to the system. The sensing material is coated between two or more IDEs, the initial resistance between these electrodes is measured before and after the exposure to the analyte. Similar to SAWS, the sensor properties depend on the thickness, uniformity and composition of the sensing layer. These are the most commonly used sensors for eNose and portable applications. Chemirersistive sensors have widely been used in enoses for detecting different VOCs and diseases. These sensors can be either selective or non-selective and can be used with pattern

recognition techniques to detect a condition based on the different patterns generated by samples from healthy and unhealthy volunteers. Metal oxide semiconductors, graphene, functionalized graphene, graphene oxide, functionalized GNPs (f-GNPs), CNTs, functionalized CNTs, and conductive polymer composites (CPCs), have been used as sensing materials by researchers to detect VOCs and biomarkers [76] [78] [79] [80] [81] [82] [83] [84] [85] [86] [87]. These materials have been previously explored for detection of volatiles.

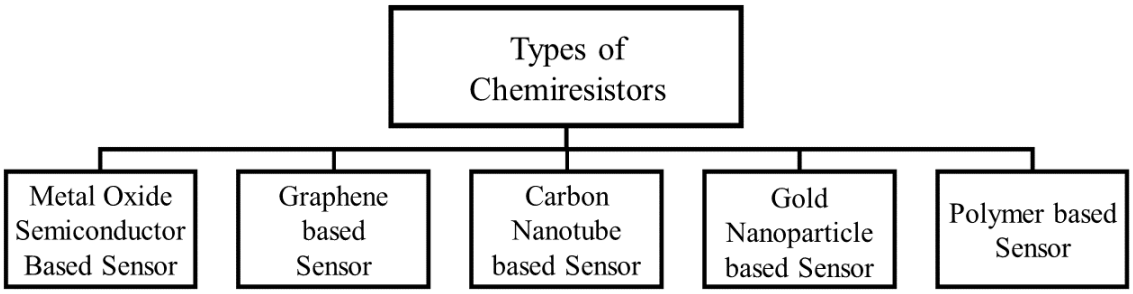

Figure 2.6. Types of Chemiresistors

Metal Oxide Semiconductor Sensors (MOS)

Based on the type of metal used, MOS devices are divided into transition and non-transition sensors. These are mostly used in indoor air monitors and fire or smoke detectors and other applications due to their low cost and high sensitivity. The MOS platform has been used to detect low concentrations (mid part per billion or ppb) of naphthalene, benzene, ethanol and benzaldehyde at high temperatures (300-500°C) [88] [89]. The poor selectivity, low stability and reproducibility are among the challenges that impact performance of MOS sensors for VOC detection in high humidity environments such as human breath.

Graphene Based Sensors

Graphene and graphene oxide are widely used in wearable and sensor technology due to their robust mechanical and electrical properties. The use of reduced graphene oxide to detect hazardous gases like NO_2, H_2 S, SO_2 and NH_3 has been reported by Sign et al. and Lu et al. [90] [91]. The drawbacks with these sensors are that pure graphene is difficult to synthesize and the sensors show low selectivity at smaller concentrations compared to graphene oxide. However, the high sensitivity of graph oxide to water vapor limit its application in detecting VOCs in human breath. Decoration of graphene with nanoparticles and functionalizing the nanosheet has been used to enhance the sensitivity and selectivity of the graphene-based sensors.

Carbon Nanotube based Sensors

CNTs are popular components of sensing application due to their electronic properties and ability to respond to different analytes based on chemical structure and functionalization. CNTs can be either single walled (SWCNTs) or MWCNTs. SWCNTs have a simple cylinder like structure and have three basic designs known as armchair, chiral, and zigzag. MWCNTs can either have a Parchment model (like a scrolled up graphene sheet) or russian model (multiple CNTs one over the other). While both types of CNTs have similar properties, MWCNTs are difficult to manufacture, MWCNTs have complicated mechanism behind response to gas adsorption and have shown high sensitivity to specific gases. Both types of CNTs have been previously used for VOC detection [92] [93]. It has been used to detect non-polar and polar analytes by Chatterjee et al. and Zilberman et al [94] [95]. VOCs such as hexane, decane, and dimethyl benzene have been detected using CNTs by Peng et al [96] These sensors, though they show promising future, currently are hindered by low response and slow desorption rate. CNT sensors presents an extremely high recovery time (near 12 hours) which limits its application for the detection of hypoglycemia [93].

Gold Nanoparticle-based Sensor

The use of GNPs as a sensing material was first published by Wohltjen and Snow in 1998 [97]. GNPs have very fast response and high sensitivity for low concentration of gases which makes this platform ideal for VOC detection [98]. The properties of these sensors can be modified by changing their shape [99], size of the core [100], length of tail group [101] and functionalized group caoting. The sensing mechanism can be explained by the effect of electron tunneling. The polymeric sensing element changes volume when they come in contact with the analyte gas due to adsorption, leading to changes in the gaps at the polymer-nanoparticle interface. This makes electron flow more difficult and thus changes the resistance of the sensor [102]. GNPs are very widely researched for VOC and chemical vapor detection by researchers and are typically decorated with different functional groups to selectively bind different VOC analytes of interest [99].

Polymer based Sensors

Polymer based sensors are low cost, low power and have varying selectivity and sensitivity based on the chemical composition of the polymer layer. The analyte interacts with the polymer layer based on either hydrogen bonds, dipole/dipole interaction or diploe/induced dipole interaction. These are very useful for low concentration VOCs that cannot be detected using MOS sensors as the polymer film can be functionalized for the specific VOCs. The two-basic type of polymer based sensors are:

1. Intrinsically Conducting Polymers (ICPs): ICPs are polymers with pi bonding that makes these polymers conductive. Generally do not have high sensitivity and also suffer from low lifespan and temperature stability. Jiang et al [102] have tested Poly(3,4-ethylene-dioxythiophene)- poly poly(styrene sulfonate) nanowires sensors to detect ketones, alcohols, alkanes and aromatic compounds. Even polymers like

polyaniline/polypyrrole composite and Polyipphene have been reviewed for sensing application with a reasonable explanation for sensing mechanism [103].

2. Conducting Polymer Composites (CPCs): Because there are not many conductive polymers available for sensor fabrication, non-conducting polymers can be used by synthesizing composites through a solvent and a conducting material. Overall, composite materials give good conductivity as well as high selectivity and sensitivity. Researchers have reported a number of CPCs including polycarbonate or PC in CB and CNTs, MWCNTs in poly(vinylidene fluoride)(PVDF), amine functionalized polyaniline, and O-phenyl diamine or OPD for the detection of gases like toluene, cyclohenexe, acetone, acetaldehyde, formaldehyde, ethanol, and methanol [104] [105] [106] [107]. Polyetheramide or PEI is another polymer that can be used to detect aldehydes [87]. However, Very few researchers like Aberici et al and Deng et al have worked on PEI sensors [108] [109]. Instead, common use of PEI has been VOC and gas removal from mixture [110] [111] [112].

2.4 Sensor Fabrication

Chemiresistive sensors are fabricated by depositing a thin layer of functional material like metal oxides, polymer composites, GNPs, and others. The substrate with interdigitated electrodes is commonly manufactured using the process of photolithography.

2.4.1 Photolithography

Photolithography is a process in which an arbitrary pattern is transferred onto a substrate following a series of steps. The conventional process uses ultraviolet (UV) radiation to transfer the pattern from an opaque and transparent mask onto a substrate covered with UV sensitive polymer called photoresist. The process is very accurate and reproducible, making it the most commonly used device fabrication method for semiconductor devices like integrated circuits, microprocessor chips and

electrodes for sensors [87] [113] [114]. The conventional process of photolithography is described below. The substrate on which the pattern needs to be transferred is cleaned and coated with photoresist. There are wet and dry photoresists available and a suitable photoresist must be used considering factors like type of substrate, accuracy, and precision required. Researchers are working on innovating new methods for photoresist deposition and photoresist synthesis [115] [116] [117]. The material is exposed to UV light through a mask made up of opaque and transparent areas forming a pattern that is to be transferred. The resolution and precision can also be altered based on type of contact between the mask, substrate and the UV source [118] [119]. After exposure, the substrate is washed to dissolve UV affected photoresist. The photoresist protects the pattern while etching, after etching the protective layer of photoresist is removed to obtain the desired pattern. The etch time is a critical parameter and needs to be optimized for any given pattern in order to achieve the desired accuracy.

Synthesis of a thin sensing layer of polymer over interdigitated electrodes is required to fabricate sensors and the sensing properties often vary based on the thickness of the film due to chemical changes that occur when chemical deposition of liquid material undergoes solidification. GNPs are generally drop cast since the randomness of drop casting improves the sensitivity of the sensing film.

2.4.2 Thin Film Fabrication

Most commonly used thin-film fabrication techniques are presented and discussed. Each thin film fabrication method has its advantages and disadvantages based on the critical parameters which are also mentioned below.

Dip Coating

This traditional film fabrication technique uses a simple process of dipping the substrate into a chemical solution. There are three steps in the processes, which

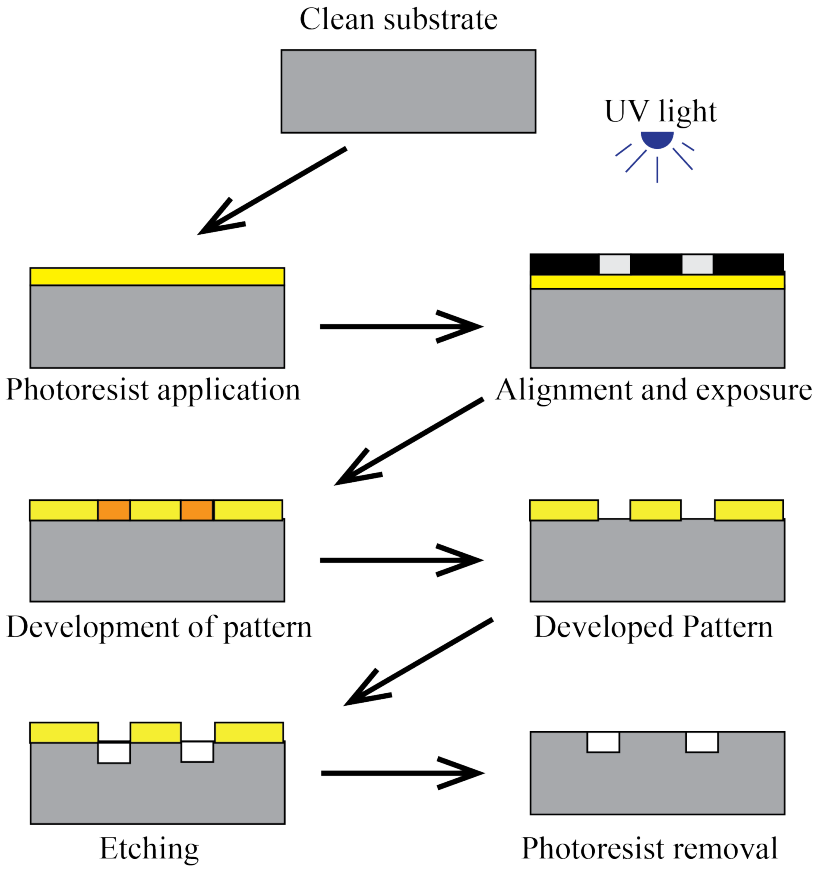

Figure 2.7. Steps Involved in Photolithography

are (1) immersion into the chemical solution for a certain time (2) pulling out the substrate at a uniform speed, letting the excess drip down (3) evaporating the precursor from the solution to form a thin layer on the surface of the substrate. The film thickness depends on factors including immersion speed, dwell time, solution concentration, evaporation environment and other parameters.

Langmuir-Blogdett (LB)

Here the substrate is dipped into a clear liquid, with high surface tension, containing a monolayer of an insoluble material is transferred to the substrate or the surface of the liquid. The material adsorbs onto the substrate due to the attraction between

the substrate and the hydrophobic monolayer tail being more than the attraction between hydrophilic head and surface of a liquid. Only insoluble polymer layers can be formed with this method. A sophisticated setup and calculations are required for using this technique.

Blade coating

This method uses a simple technique of moving a thin-edged knife over a substrate after putting a drop of precursor to be coated over the substrate. A thin uniform layer forms over the substrate and the film thickness depends on the distance between knife and substrate, knife speed, viscosity, density, and other properties of the chemical.

Chemical Vapor Deposition

In this process, the heated substrate is exposed to precursor gas in a vacuum environment. A catalyst can be used to enhance the process. A thin layer of a precursor is formed over the substrate as it cools down. Gas flow is also used inside the vacuum chamber to carry out the by-products of the process. This results in a very thin layer (few nanometers) over the substrate.

Spin Coating

Here the substrate is fixed on a rotating chuck and is covered in excess coating material, before rotating it slowly to spread the material evenly, and then at high speed to form a thin layer. Various factors like material properties, spin speed, and spin time affect the thickness and uniformity of the film. The simplicity, ease of set-up, and uniformity achieved make it more suitable for polymer layer formation. It is a benchmark for process for thin film fabrication in industry and in academia. The thickness is inversely proportional to the square root of spin speed or angular velocity.

2.5 Sensor Integration System Development

Sensors are generally tested in the laboratory using a semiconductor characterization instrument. However, in order to implement the sensors in the desired application, a sophisticated sensor interface circuit is required to convert the sensor signal into useful data by signal processing. For gas sensors, the system should be able to filter, amplify and read the sensor signal to detect the concentration of the gas in the sample and then communicate the results. The eNoses commonly uses these interface circuits for signal conditioning and amplification. Most of these systems are for general purposes and can perform a variety of different analyses on a variety of different compounds. These are low cost and fast solutions for many situations but due to their limited capability, they are not suited for application in disease diagnosis and biomarker detection. Researchers are currently developing more targeted and specialized systems for applications including emission control, leak detection, food quality analysis, plant health detection and others. Rapid progress in nanomaterial synthesis, fabrication technologies, and electronic systems is enabling the development of targeted systems. These devices commonly use a single type of transduction mechanism and are very bulky and have a very long processing time. The signal from the gas sensors is usually a change in resistance that can either be processed as a voltage (digital or analog), frequency, or pulse width. The pulse width modulated (PWM) signal is generated based on resistor-capacitor charge-discharge delay occurring due to a change in sensor resistance. PWM based interface circuit is more suitable for metal-oxide-semiconductor sensors as it is convenient to combine with a heater circuit for temperature control that is necessary for MOS sensors [120] [121] [122]. Converting signal into PWM is complicated, limits the sensitivity and resolution by digitalizing large baseline value, and requires complex circuitry [123]. Conversion to voltage can be achieved using a voltage divider or a Wheatstone bridge. Sometimes the differential voltage is converted from analog to digital, this limits the dynamic range of the system and increases power consumption due to more number of com-

ponents used [124]. Digitalizing the signal also makes the system unstable due to bit-fluctuation with noise created by chemiresistors [125]. While voltage divider or a half-bridge is very simple, it can be affected by temperature and are not very sensitive to small changes, the figure 2.8 describes how voltage divider works [126]. The voltage divider also shows a non-linear response when the driving voltage is constant [127]. Wheatstone bridge eliminates the effects of change in temperature and power source parameters due to its symmetry [128]. Wheatstone bridge has been a popular method since its discovery, researchers have used it for chemiresistors before [125] [129] [130]. The sensitivity of the wheatsone bridge circuit is given by 2.1 where R and δ R are sensor resistance and change in sensor resistance respectively and V_in and V_out are voltage input and voltage output.

$$Sensitivity = \frac{V_{out}/V_{in}}{\Delta R/R_0} \tag{2.1}$$

If all four arms of the wheatstone bridge are different then the voltage output of the bridge is given by 2.2

$$V_{out} = V_{in} \times \frac{\frac{R_3}{R1} - \frac{R4}{R2}}{(1 + \frac{R_3}{R_1})(1 + \frac{R_4}{R_2})} \tag{2.2}$$

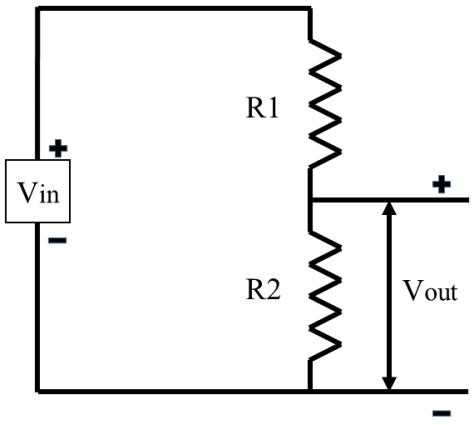

Figure 2.8. Circuit Schematics for Voltage Divider

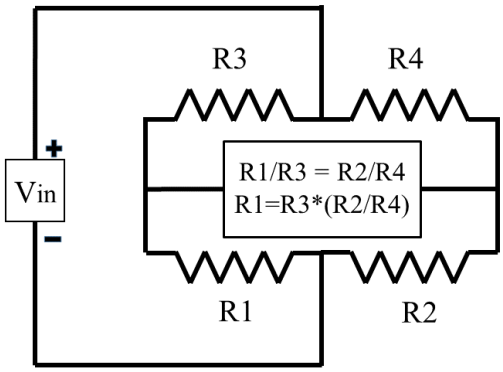

Figure 2.9. Circuit Schematics for Wheatstone Bridge

The portable sensor system also consists of a communication module that can communicate the sensor results with external devices like smartphones and computers. The commonly used wireless communication tools for sensor systems are Bluetooth, ZigBee, and Bluetooth Low Energy (BLE). The use of Bluetooth is not preferred in portable systems due to its high power consumption. ZigBee requires less power but the communication over ZigBee is not secured. BLE, on the other hand, is secured and it uses low power, making it an ideal communication tool for this project.

2.6 Multivariate Statistical Analysis for Identifying Breath VOCs

Weather the samples are analyzed by GC-MS or using a sensor, the data needs to be statistically filtered and analyzed to make a conclusion. Multivariate analysis targets multiple features, as opposed to univariate analysis that targets single feature, from the data that can best classify the sample classes (healthy from diseased). The most common unsupervised and supervised methods used for multivariate statistical analysis of breath data are described below.

2.6.1 Principle Component Analysis (PCA)

PCA is an unsupervised multivariate statistical analysis method that transforms the original data into orthogonal dimensions where the new data presents maximum variation within all samples across the new dimensions. This is mostly implemented as a preliminary analysis that is used to validate the data, identify outliers, and delineate classes. PCA has also been used to reduce the dimensionality of the data by ignoring the data with small variation in the new dimensions. The axes with maximum separation are selected as PC1. For plotting purposes, two or three components/axes are used while cross-validation is required to determine the number of axes for data modeling [131]. Researchers have used PCA with GC-MS data to illustrate separation between breath samples from diseased patients and healthy controls for colorectal cancer, head, and neck cancer, lung cancer, and type 2 diabetes [132] [133] [134] [135] [136]. PCA has also been implemented on eNose data for wine classification, tea quality identification, and vinegar sample discrimination [137] [138] [139].

Consider a data matrix X of n x p dimensions, for a dataset of p numerical variables and n entities for each variable. PCA seeks a linear combination of the variables of matrix X that has maximum variations (expressed in equation (2.3)) [140].

$$\sum_{j=1}^{p} a_j \; Xj = Xa \tag{2.3}$$

$$var(Xa) = a^T Sa \tag{2.4}$$

Where a is a constant vector. The variance is given as equation (2.4) with S being the sample covariance matrix for the dataset. In simpler terms, find p-dimenstional vector a that maximizes $a^T Sa$. This can be reduced to 2.5. That implies that a is an eigenvector with eigen values λ for covariance matrix S [140].

$$Sa \; - \; \lambda a = 0 \iff Sa \; = \; \lambda a \tag{2.5}$$

$$Xa_k \; = \; \sum_{j=1}^{p} a_{jk} \; Xj \tag{2.6}$$

Using the Lagrange multipliers approach and applying the condition of orthogonality, the equation (2.3) can be transformed to 2.6 [140]. The solution Xa_k (linear combinations of a_k) are known as principle components and the elements of these components are known as PC scores. The theory is described in detail by Ian T. Jolliffe, Jorge Cadima [140].

2.6.2 Linear Discriminant Analysis (LDA)

LDA is similar to PCA, but LDA is supervised and transforms the data to maximize the distance between means of two identified classes and minimize the scatter. Supervised methods such as LDA take into consideration the class labels (control, diseased, and other). It is widely used for dimensionality reduction in biometrics, chemistry and other fields that require the proper handling of big data. There are three steps in LDA, first one is to calculate the separability (between class variance), second one is to calculate scatter (within class variance) and third step is to formulate a lower dimensional space [141]. LDA has been used on GC-MS and eNose data for multiple applications like cigarette smoker breath sample discrimination, hypoglycemia detection from breath sample, lung cancer tissue analysis, chinese liquor classification, and coffee classification [6] [142] [143] [144] [145].

In summary, LDA projects the data onto a lower dimensional space by calculating and maximizing between class variance and within class variance. Between class variance is calculated using 2.7 [141] where m_i is the projection of the i^th class mean, m is the total mean projection, W is the transformation matrix, and μ_i and μ are actual i^th mean and total mean. Within Class variance (S_{wi}) is calculated using 2.9. Where x_{ij} is the i^th sample of j^th class, d_j is the centering data for j^th class. The total within class variance is the sum of all within class variance (equation 2.9) [141].

$$(m_i - m)^2 = (W^T\mu_i - W^T\mu)^2 = W^T(\mu_i - \mu)(\mu_i - \mu)^T W \tag{2.7}$$

$$\sum_{j=1} (W^T x_i \ - \ m_j)^2 \ = \ \sum_{j=1} W^T S_{Wj} W \tag{2.8}$$

$$S_W \ = \ \sum_{j=1}^{3} S_{Wi} \tag{2.9}$$

The lower dimensional space is constructed using Fischer's criterion and is described in eqYY3, the eigenvalues for the transformation matrix W are represented by λ. The solution is obtained by formulating the eigenvalues [141].

$$S_W \ W \ = \ \lambda \ S_B \ W \tag{2.10}$$

The literature review suggests that the currently available devices for detection of hypoglycemia are mostly invasive and mentally stressful. The VOC research is promising and suggests that there are VOC biomarkers available in breath for noninvasive detection of hypoglycemia. Though the eNose technology is promising, it is not portable and uses the black box approach. Additionally, the sensing technology available is inefficient to detect the VOCs in breath due to the high humidity and the system is not customised for medical use. This serves as a motivation for this research project, to design and develop a portable sensor system for noninvasive detection of hypoglycemia.

3. MATERTIALS AND METHODS

Material and methods used for fabrication and development of nanosensor array are presented. This includes synthesis of sensing material, fabrication of interdigitated electrodes (IDEs), fabrication of sensor array, fabrication of signal conditioning circuit, and experimental testing methods are described. Statistical analysis used to determine and validate the biomarkers of hypoglycemia is presented in Section 3.1. The material used for the development of the sensors and the electrical interface circuit is provided in Section 3.2. Fabrication of sensors and the sensor array are described in Section 3.3. Design, fabrication and the development of the electrical interface circuit (signal conditioning circuit) is presented in Section 3.4. The experimental testing set up and the sensing mechanism of the proposed sensors are described in Section 3.5.

3.1 Statistical Analysis of the Breath data Analyzed via GC-MS

Five Adult patients with type 1 diabetes were recruited through the IU Health System according to a process approved by the Indiana University Institutional Review Board for the stepped hypoglycemic glucose clamp procedure. The patients donated breath bags were analyzed by GC-MS (Agilent 5975C mass spectrometer,City, Country) using Siloxane fiber (Superlco, Bellefonte, PA, USA). Raw data obtained from GC-MS was deconvoluted with help of Automated Mass spectral Deconvolution and Identification System or AMDIS software [146] and spectral alignment was performed using the SpectConnect server at Georgia Institute of Technology, which identifies the components automatically [147]. The output from SpectConnect were two matrices containing spectrally aligned components with integrated signal (IS) value and Retention time (RT) value. The data was screened for components that were obviously exogenous, had bad retention time, and were not present in 50% of the sample set.

An iterative LDA method was implemented to identify a small panel of VOCs that relates to hypoglycemia. The details for this simple computational feature selection are described elsewhere [6]: it first determines the specificity, sensitivity, and area under the curve (AUC) of a receiver operating characteristic (ROC) curve for a combination of three VOCs. Next, using the pre-generated IS matrix, all possible combinations of three VOCs are tested to identify the group that presents the highest AUC. These three VOCs are used for iteratively trying combinations of four and then five VOCs, and the process is repeated, until a best combination is obtained for the specificity, sensitivity, and AUC. To check the model for overfitting, results are subjected to cross-validation, deterioration of cross validated results is an indication for overfitting. This leads to an identification of the simplest combination of metabolomics biomarkers or VOCs that provides strong predictive outcomes. Cross-validation of results were obtained using with MATLAB classifier app, specifically, 10-fold validation with linear analysis. The method is described in detail elsewhere [148].

3.2 Materials

Silicon wafers coated with Silicon Dioxide (SiO_2 - 300 nm), Chromium (Cr-5 nm), and Gold (Au- 90 nm) respectively were procured from Hionix Inc (San Jose, California, USA) for making the interdigitated electrodes for the sensors. S1813 positive photoresist (MicroChem Laboratory, Round Rock, Texas, USA) and an adhesion promoter MCC Primer (80/20) (MicroChem Laboratory, Round Rock, Texas, USA) were obtained for photolithography. For development, microposit MF-321 developer (Rohm and Haas Electronic Materials LLC, Marlborough, Massachusetts, USA) was used. Gold etchant and Chromium etchant was procured from Sigma Aldrich (St. Louis, Missouri, USA). The f-GNPs were purchased from Sigma Aldrich (St. Louis, Missouri, USA), along with PEI, 1-Methyl- 2-pyrrolidinone (NMP), polyethylene oxide (PEO), and other reagents. Carbon black (Black pearl 2000) was obtained from Cabot Corporation (Boston, Massachusetts, USA). PVDF-HFP (FLEX 2801 PVDF)

was obtained from Arkema Group (Colombes Cedex, France). Diethylene carbonate (DEC) was procured from Novolyte Technologies (Zachary, Louisiana, USA). Dry medical air and Pure Nitrogen was purchased from Praixair (Danbury, Connecticut, USA). The components used for the interface circuit were purchased from DigiKey (Thief River Falls, Minnesota, USA). All the resistors are surface mounted or SMDs with size specification 1206 (120mils length by 60mils width). The microcontroller used is Arduino Bluno nano (SKU DFR0296, purchased from Digikey) with onboard BLE from DFROBOT (Bluno).

3.3 Fabrication of Sensor Array

3.3.1 Synthesis of Sensing Material

PEI: PEI comes in small pallet form and are clear-yellow in color. To remove the moisture, the polymer was stored in vacuum for 48 hours. This PEI was then dissolved in NMP in a ratio of 1:3 by stirring the mixture at 800C for at least 48 hours.
PVDF-HFP: The solution was made in similar way by adding PVDF-HFP powder in NMP (1:5). 2% glycerol (w/w) was added to this solution to enhance the composite uniformity.
PVDF-HFP/CB: The solution was made with PVDF-HFP powder in NMP (1:5). 5% Carbon black (CB) was added to this solution that makes the polymer layer conductive. The concentration of carbon black was optimized to get better sensitivity.
PEO/DEC: PEO and DEC were sonicated to get mixture of PEO and DEC (4:1% w/w) that was used for modifying properties of sensing film.

3.3.2 Fabrication of Interdigitated Electrodes (IDEs)

IDEs were fabricated over gold and chromium coated Si/SiO_2 substrate using a traditional photolithography process with the help of OAI series 200 Mask Aligner and Exposure system. The figure 3.1 shows the picture of the instrument. The mask

for photolithography was designed on Coventor Ware 2012 and was procured from Louisiana Tech University, printed on a glass substrate. The design in shown in 3.1. As seen in the figure, the mask design is printed on glass with high-resolution printers. It is important to make sure that the mask is manufactured without defects as the defects can be reflected in all the products.

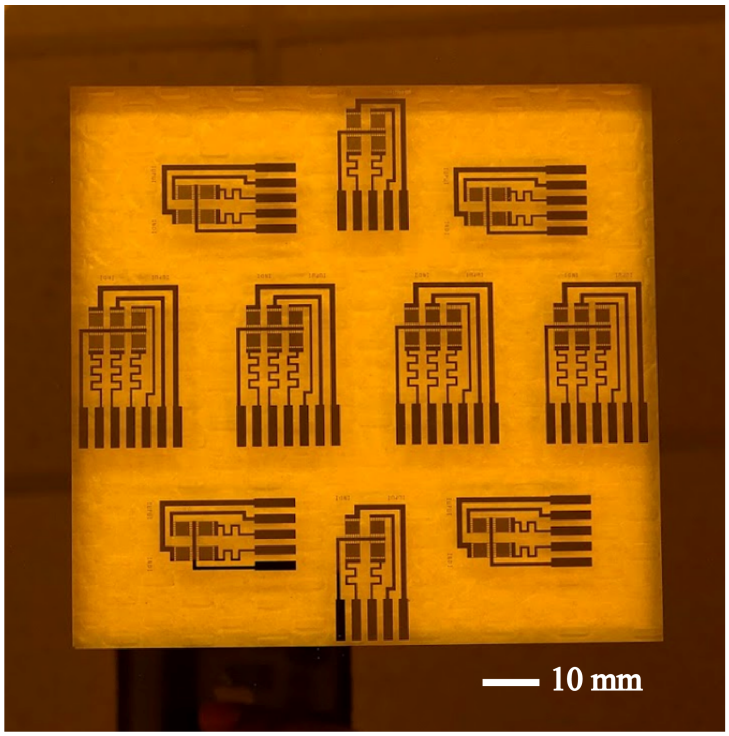

Figure 3.1. Picture of Mask Design Printed on Glass

Photolithography Process

The Si/SiO_2 substrate was cleaned thoroughly with acetone, ethanol, isopropanol (IPA) and then with high pressure DI water to remove any dust particles or residues. To evaporate any solvents left after cleaning, the substrate was dried with medical air and then heated 90°C for 5 minutes. The surface was then spin coated with adhesion promoter MCC Primer 80/20 at 500 *rpm* with spread time of 5 *s* and at 3000 rpm

with spin time of 40 s. The primer helps in adhesion of photoresist to the gold surface of substrate. Various factors like spin speed, spin time viscosity ofphotoresist are responsible for thickness of photoresist film over substrate. The photoresist S1813 was coated at 3500 rpm for 40 s. The substrate is soft baked at 90°C for 15 s. The higher temperature or longer exposure to heat can cause cross linking or decomposing of photoresist. The exposure time was optimized to 4.6 s for the 5μm-8μm electrode gap.

After exposure the mask was developed with Miroposit MF-321 for 1 minute while

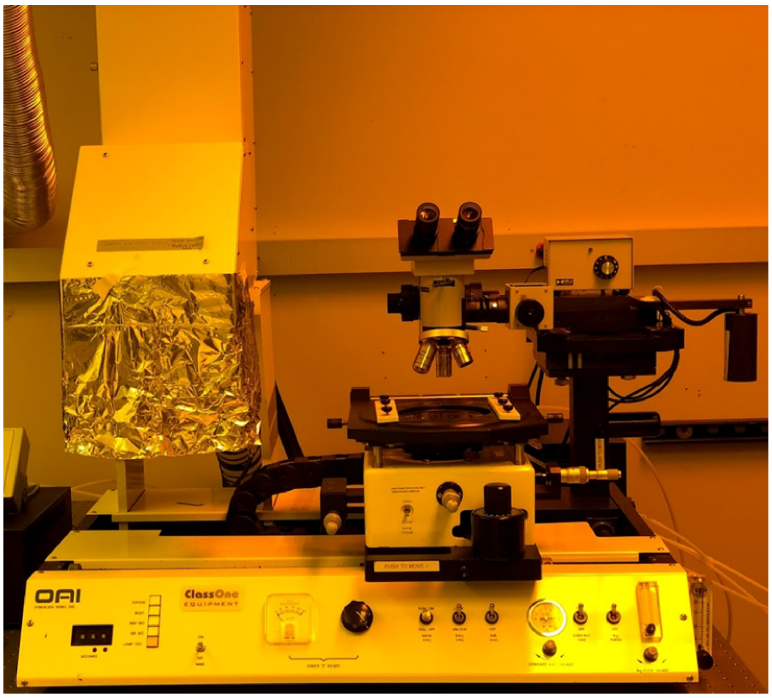

Figure 3.2. OAI Series 200 Mask Alignment and Exposure System

shaking. The over exposure or under-exposure can cause damage to the pattern. After development the substrate was cleaned with water and hard baked at 90°C for 10 minutes. The optical inspection was performed using optical microscope to make sure the pattern was developed properly. The substrate was then etched with gold etchant for 30s in glass. The substrate was then cleaned and washed with water and air to remove etchant residues since it reacts with chromium etchant used in

next step. Similar process was followed for chromium etchant with etch time of 20s. To remove the layer of photoresist, the substrate is cleaned with acetone, ethanol, and IPA. Final inspection for defects, impurities and dimensions was performed to optimize the process. A fabricated IDE and the mask used for its development are shown in the figure 3.3. The average gap between the electrodes is measured to be between 8 μm which is shown in inset of figure 3.3

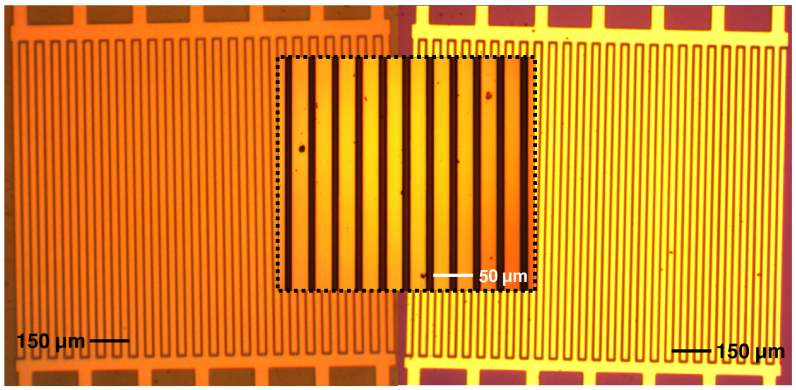

Figure 3.3. IDEs from Mask on Left Compared to IDEs After Etching on Right with Inset Showing Gap Between the Electrodes

3.3.3 Fabrication

An array of sensors was fabricated over three separate substrate of containing IDEs of gold patterned over Si/SiO_2 substrate. The sensor array were composed of sensors of polymer/f-GNPs and polymer/CB. More specifically, sensors of PEI-EGNP (4 sensors), PVDF-HFP-EGNP (4 sensors) and PVDF-HFP/CB(4 sensors) were successfully fabricated and tested with the targeting VOCs.

Fabrication of Polymer/f-GNP Sensors

The drop casting method was used to fabricate both E-GNP sensors over IDEs with a 5-8 µm gap. The sensors were dried in vacuum for 48 hours. The method is known to give better sensitivity due to the non-uniform distribution of GNPs. The sensors were then coated with a thin polymer layer using a spin coating fabrication method.

A thin layer of PEI and PVDF-HFP were formed over E-GNP sensors giving two sensor arrays. PEI layer was formed using spin coating at 6000 rpm for 1 min after spread speed. The substrate was heated at 800C for 150 seconds to evaporate the excess solvent and for a thin polymer layer. The sensors were stored in a vacuum for next 48 hours before testing. A thin layer of PVDF-HFP was spin coated at 4000 rpm for 1 min. The film was then stored in a vacuum for drying without heat treatment.

Fabrication of PVDF-HFP/CB Sensors

The sensor was fabricated by spin coating polymer layer directly over the IDEs. The speed of 3500rpm was used for 55 s to get uniform film thickness. The sensor was dried at room temperature for 18-24 hours before removing the excess solvent and glycerol through a water bath procedure. The sensor was then stored in a vacuum for over 24 hours before testing. The sensor was sensitivity and selectivity was enhanced by treating the polymer composite using PEO and PEO/DEC layer deposition (drop casting) [86].

3.4 Experimental Setup and Sensing Mechanism

The sensors were tested in four different ways, first with individual VOCs, then with multiple VOCs (combinations of 2 and 3 VOCs), and with Simulated breath. For these tests, a dedicated sensor testing setup was built. Dry medical air (76.5%-80.5% Nitrogen, 19.5%-23.5% Oxygen) was used as a carrier gas for experiments to avoid any

interactions from the atmosphere. Mass flow controllers (Alicat scientific, Marana, Arizona, USA) were used to bubble controlled flow of air through liquid VOC and get VOC vapors in the carrier gas. The sensor was sealed inside a testing chamber with 300 cc volume to avoid any interaction with atmosphere. The carrier gas along with VOCs was introduced for a fixed time into the chamber after letting the sensors get stable to the dry air. To test the sensors at different concentrations, the flow rate was varied. The total flow was kept constant to 400 standard cubic centimeters per minute ($SCCM$) for individual and multiple VOCs. The flow was kept at 1000 $SCCM$ for simulated breath. The average flow for human breath when asked to blow into the bag is around 0.2 liter/second i.e. 1200 $SCCM$. The sensor results with standard deviation errors are presented in the results Section. The sensors are tested with VOC1, VOC2, VOC3, VOC4 to check sensitivity and selectivity. The sensor is tested with simulated breath at 93% relative humidity (RH) for 30s cycles. Simulated breath refers to a mixture of high humidity with dry air, VOC of interest and a small amount of acetone and ethanol.

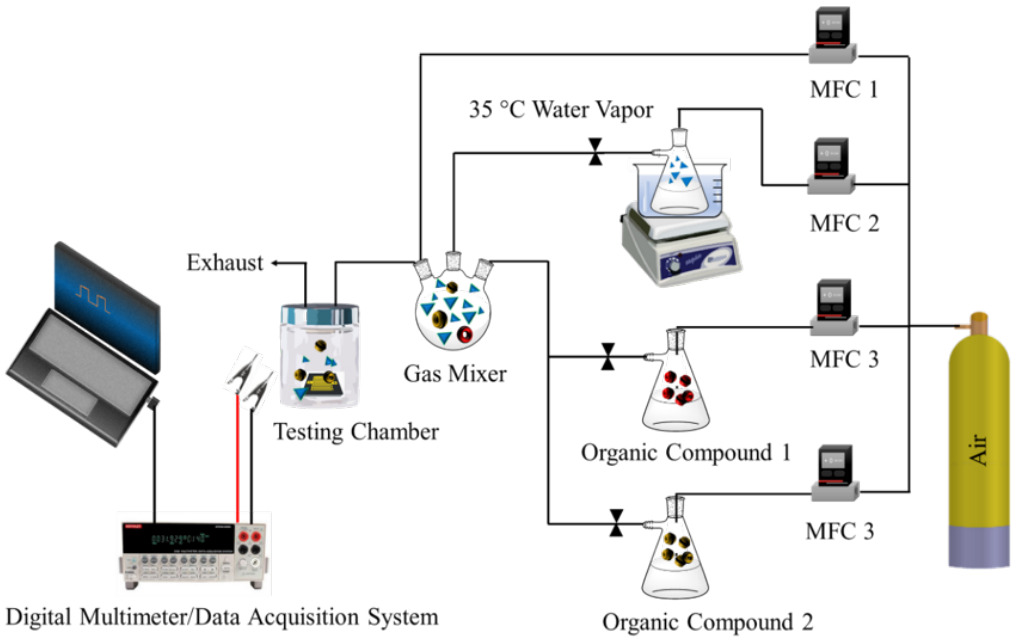

Figure 3.4. Experimental Setup Used for Testing the Sensor Arrray

The experiments were conducted at room temperature ($21°C$- $25°C$). The temperature for simulated breath was adjusted to $35°C$ to match with human breath. RH was validated using a commercial humidity sensor (CO_2 meter, City, state, Country). The concentration of VOCs in parts per million (ppm) was calculated based on the following 3.1 The resistance and change in resistance were measured fusing Keithley 2701 Digital Multimeter/ Data Acquisition/ Data Logging system (Beaverton, OR, USA). The data was logged using Keithley KickStart software on a computer with RS232 interface. The logged data was stored in excel file and was analyzed using Microsoft Excel.

$$Concentration\ (ppm) = 10^6 \times \frac{Vapor\ Pressure\ _{VOC}\ (mmHg)}{760} \times \frac{MFC\ _{VOC}}{MFC\ _{total}} \quad (3.1)$$

Sensing Mechanism

There is literature available describing the sensing mechanism of the f-GNPs based on the quantum tunneling effect [57], [149]. The VOC analytes interact with f-GNPs and alter the network formed, affecting the electron tunneling that transports the electrons between electrodes [150]. The electron tunneling resistance (R_t) is given as [151] [152]:

$$R_t \propto exp(\beta L) \times exp(\frac{E_A}{kT}) \quad (3.2)$$

Where,

L= average separation gap between nanoparticles,

β = electron tunneling decay constant (depends on thiol matrix),

E_A = activation barrier energy,

k = Boltzmann constant,

and T = temperature

When the analyte molecules interact with thiols (adsorbed on sensor surface), it causes swelling of thiols that changes the gap between GNPs and causes change in resistance. So the relative change can be given as:

$$\frac{\delta R}{R_0} = \frac{R(L+\delta L) - R(L)}{R(L)} = exp(\beta \delta L) - 1 \quad (3.3)$$

As the equations suggest, particle size and surface characterization plays an important role in sensing. The presence of double bonded oxygen makes the EGNP more sensitive towards hydrogen donor compounds like alcohols, aldehydes and alkanes. The lone pair from double bonded oxygen initiates the hydrogen bonding with various gases. The polymer film was deposited over it to modify the selectivity and sensitivity of the sensors and enhances the sensor stability in harsh environment such as human breath. The structure of these GNPs is shown in figure 3.5.

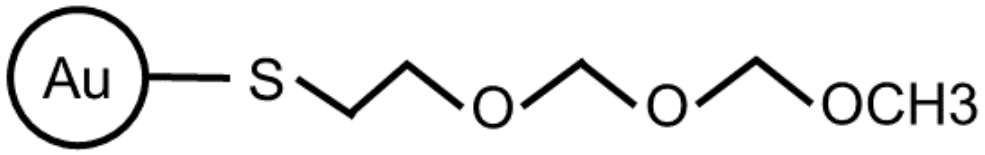

Figure 3.5. Structure of 1-Mercapto-(triethylene glycol) methyl ether functionalized gold nanoparticle

For the polymer composites, the sensing mechanism can be explained with the help of a phenomenon known as percolation theory. The polymer matrix, in this case PVDF-HFP matrix is non-conductive. Carbon black, a conductive material is infused inside the polymer matrix to make the polymer conductive. When there is just enough conductive material inside the polymer matrix, the polymer can transfer electrons with small resistance. When this CPC matrix interacts with VOCs, the polymer expands and the distance between the conductive particles increases, causing the resistance to increase. The ratio of materials is very crucial as the percentage of conductive material inside the matrix translate into sensitivity.

3.5 Fabrication of Sensor System

The interface circuit was designed on Autodesk Eagle PCB Design Software, analyzed on OrCAD PsPice Simulation, and fabricated on a printed circuit board (PCB).

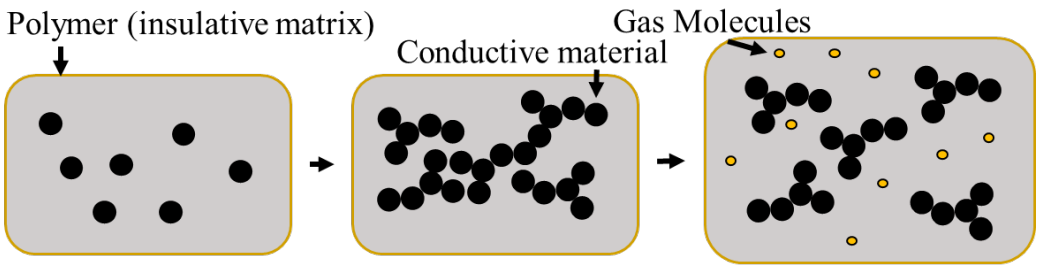

Figure 3.6. Percolation Theory of CPCs

3.5.1 Interface Circuit Design Considerations

The interface circuit is required to connect the sensor to the microprocessor as a microprocessor is mostly incapable of processing direct sensor output. The circuit was designed in three parts: A multiplexing unit that is able to select an input from number of inputs based on received signal from a processor, a signal conditioning unit to convert the change in resistance of the sensor into analog voltage value and amplify the signal to readable value for further processing, and a microprocessor that can control these components and process the signal for conclusion.

3.5.2 Design of Interface Circuit on Eagle PCB

The initial prototype was built on a breadboard and then on a general-purpose board to test for functionality.

Multiplexing Unit

Dual 4-channel analog multiplexer/demultiplexer 74HC4052D (Nexperia USA inc) (MUX) is used to switch between sensors periodically and connect each sensor to the signal conditioning and amplification unit based on digital inputs from onboard microcontroller, Bluno. S0 and S1 are digital signal inputs that are used to select the output (Z) from available 4 inputs (Y0, Y1, Y2, Y3).3.1 shows how the outputs are

Table 3.1. Multiplexer Output Selection Based on Control Input E, S1, and S0 [153]

E	**S1**	**S0**	**Output**
LOW	LOW	LOW	Y0
LOW	LOW	HIGH	Y1
LOW	HIGH	LOW	Y2
LOW	HIGH	HIGH	Y3
HIGH	X	X	None

selected. The sensors are connected to the multiplexing unit through a connector.The output from the mux is connected to a Wheatstone bridge circuit that has three fixed resistor arms.

Signal Conditioning and Amplification Unit

The resistance change of the sensor is converted into a voltage difference and is amplified using an LM324-N low power Quad- operational amplifier (Texas Instruments) (op-amp). The bridge is powered by Bluno with $3.3V$ supply while the op-amp is powered at $5V$ from Bluno. The gain of the circuit is adjusted using the combination of resistors connecting to the op-amp. Considering the 2.2, if R3 is replaced by a sensor then the output voltage of the wheatstone bridge is given my 3.4, where R3 is a variable sensor resistance. This outputof Wheatstone bridge is further supplied to differential amplifier circuit that amplifies the signal based on the gain values. The output of differential opamp circuit is given by 3.5. V^+ and V^- are the inputs to opamp and G is the gain value that is based on the resistance connected in circuit (R_f and R_x)

Microcontroller Unit

Microcontroller Unit: The Bluno nano board used in the project uses Atmega 328 microcontroller and has on-board TI CC2540 BLE chip with transmission range over 20 m that can be connected to android and iOS devices. This microcontroller board is powered by $4.8V$ battery or USB. The board is programmed using an Arduino Integrated Development Environment.

$$V_{out} = V_{in} \times \frac{R_3 \ - \ R}{R_3 \ + \ R} \tag{3.4}$$

$$V_{amp} = (V^+ \ + \ V^-) \times G \tag{3.5}$$

$$here, \ G = \frac{R_f}{R_x} \ , \ V^+ = V_{in} \times \frac{R_3}{R \ + \ R_3}, \ and \ V^- = V_{in} \times \frac{1}{R} \tag{3.6}$$

Schematic Design of Interface Circuit

Eagle PCB allows placement of different analog and digital components from the circuit on the sheet and connecting these components with wires or buses. Most of the components were already available in the eagle library and were used without modification. Arduino Bluno pinout was not available and was designed on the software for ease of fabrication using dimensions and pin diagrams available on the website [154]. The schematic design was iterated several times to optimize the circuit. figure 3.8 shows the circuit layout designed on Eagle.

Layout Design of Interface Circuit

After initial schematics design, Eagle allows users to develop a layout of the circuit on a virtual PCB. The software allows placement of components on the virtual PCB in required orientation. Connection between the components can be achieved by autorouter tool available on the software that connects the components while optimizing the space and other parameters. Compact placement of parts or complex design can cause the autorouter to keep few connections open that can be manually connected or

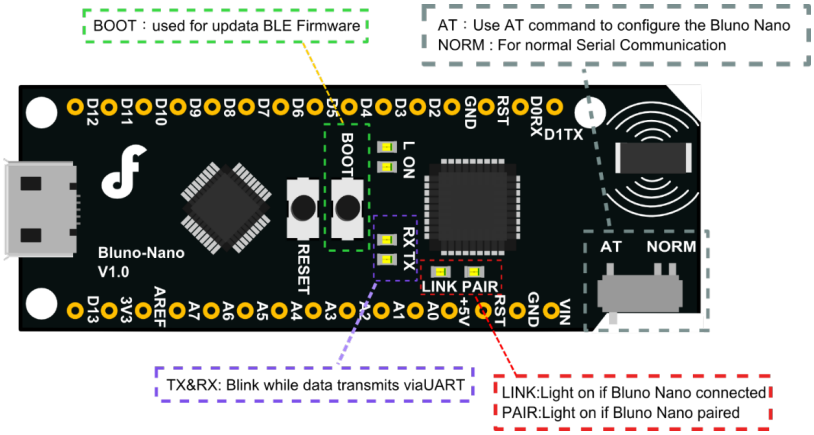

Figure 3.7. Pinout diagram of Arduino Bluno nano board [154]

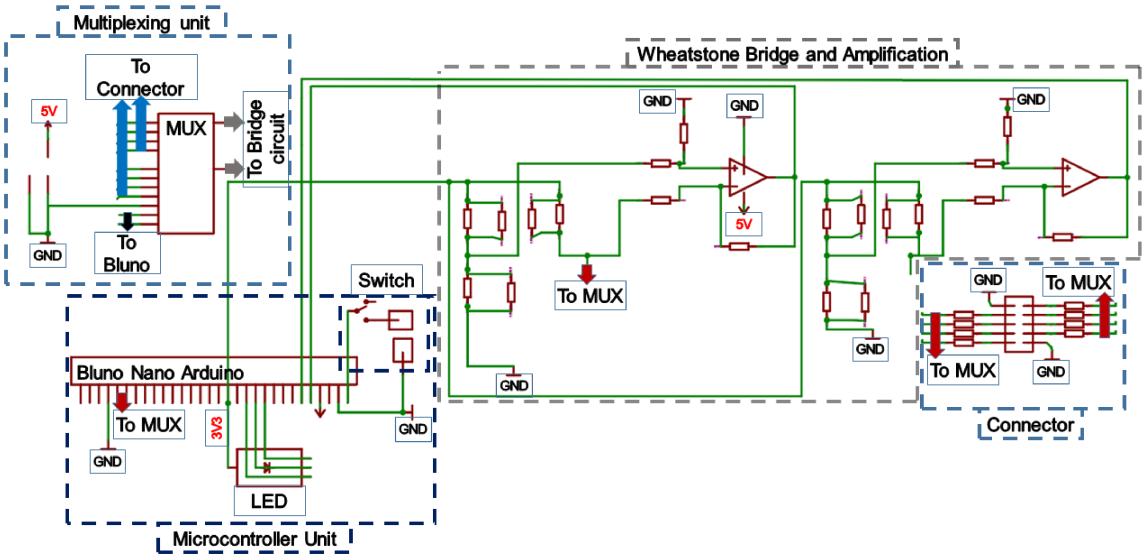

Figure 3.8. Sensor System Schematic Designed on Eagle PCB

placement of components can be updated to accommodate all the connections. The layout was designed in order to make replaceable components easily accessible. The 2 layer PCB layout is shown in figure 3.9 where the blue colored components are on the back side while red colored components and connections are on the front side.

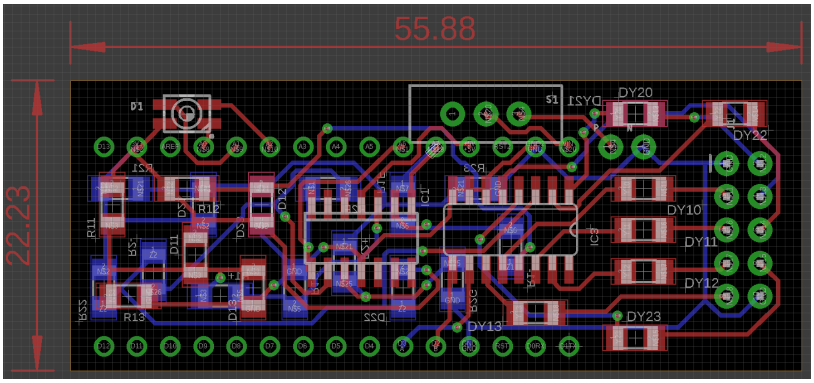

Figure 3.9. Sensor System Layout Designed on Eagle PCB

3.5.3 Fabrication of Sensor System on PCB and Design of Packaging

The PCB was printed by Advanced circuits Inc (Aurora,CO ,City, State, Country) with both side soldermask and silkscreen. The vendor requires gerber files (Computer Aided Machining files for PCB design) that the software generates using a CAM tool. Once received, all the components on the circuit were soldered at research facility.

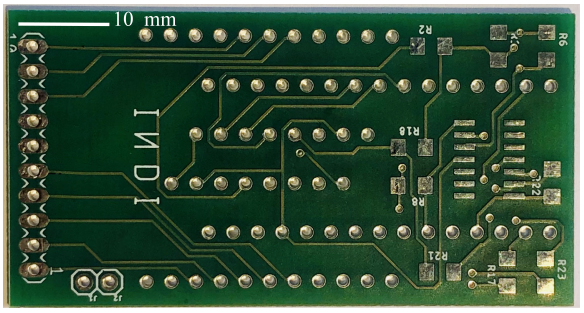

Figure 3.10. Fabricated PCB Received from Advanced Circuits

Packagining Design

Packaging for the whole system was designed on PTC Creo (MA, USA). And 3D printed from "Think It Make It" lab at Herron School of Arts and Design, IUPUI (IN, USA). The material used for packaging is polylactic acid or PLA for prototyping

purposes. The packaging can be manufactured using materials like glass, polypropylene, or silicon to avoid interaction with the sensors, caused by the degassing of the plastic. The schematic image of the designed packaging system is provided in the figure 3.11.

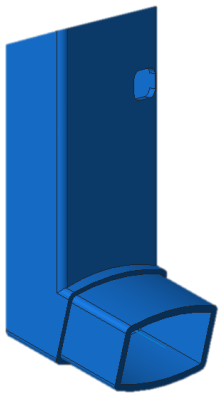

Figure 3.11. Sensor System Packaging Designed on PTC Creo 4.0

3.5.4 Programming of the Sensor System

The system was programmed using Arduino Integrated Development Environment software which uses basics of C and C++ programming language [155]. The software enables easy programming of the Arduino microcontroller. The program is not represented in the thesis. It contains the code to define all the sensor variables, collect the sensor data every 8 seconds for further data analysis. It performs matrix multiplications to extract features from the sensor data that can further scale the analysis result between one to ten, where one is Normal and 10 is Hypoglycemic. The system is also equipped with bluetooth that allows communication of the results to smartphone and computers. A multi-color LED from the system is flashed based on the results where red indicates Hypoglycemia, yellow indicates caution, and green indicates euglycemia or normal condition.

4. **RESULTS**

This Chapter describes the results for characterization and testing results of the statistical analysis, sensing material, fabricated electrical system, and fabricated sensor array. Section 4.1 describes the statistical analysis results performed on GC-MS data using MATLAB. The FESEM, UV/VIS and contact angle characterization results are presented in Section 4.2. Section 4.3 describes the PEI-EGNP, PVDF-HFP/CB, and PVDF-HFP-EGNP results tested as an array with a combination of multiple VOCs and with the simulated breath. The results with characterization and testing of the interface circuit are described in Section 4.4.

4.1 Statistical Analysis

The statistical analysis was performed on data acquired from the breath sample analyzed on GC-MS and spectrally aligned using SpectConnect server from Georgia Institute of Technology. Univariate statistical analysis identified 88 components with p-value less than 0.05 (student's t-test) between clam samples and camp samples from normalized relative abundance matrix. Further analysis of this data suggested 38 of the components/VOCs presents a statistically significant relation to hypoglycemia (RT standard deviation less than 0.5). However, none of these 38 VOCs were able to perfectly separate hypoglycemic and normal samples individually. Next, multivariate analysis was conducted to identify a combination of VOCs that can achieve the highest AUC and separates hypo samples from non-hypo samples. Using the approach of iterative LDA, described in methods, a panel of six VOCs was identified that could perfectly separate the hypoglycemic breath samples from normal breath samples, that yields 85.71% sensitivity and 100% specificity with AUC of 0.99. Belsley collinearity diagnostics ensured that there is no strong collinearity among the VOCs in the identi-

fied panel of VOCs. The VOCs were identified by NIST14 but were not verified, and the names are not disclosed herein. A representation of the LDA scores for the 25 samples is shown in figure 4.1, demonstrating perfect separation in the between samples. The results were cross-validated using the MATLAB's classification learner app (MATLAB R2018a 9.4.0.1) (10-fold cross-validation feature). The cross-validation was carried out 1000 times and the averaged data was reported.

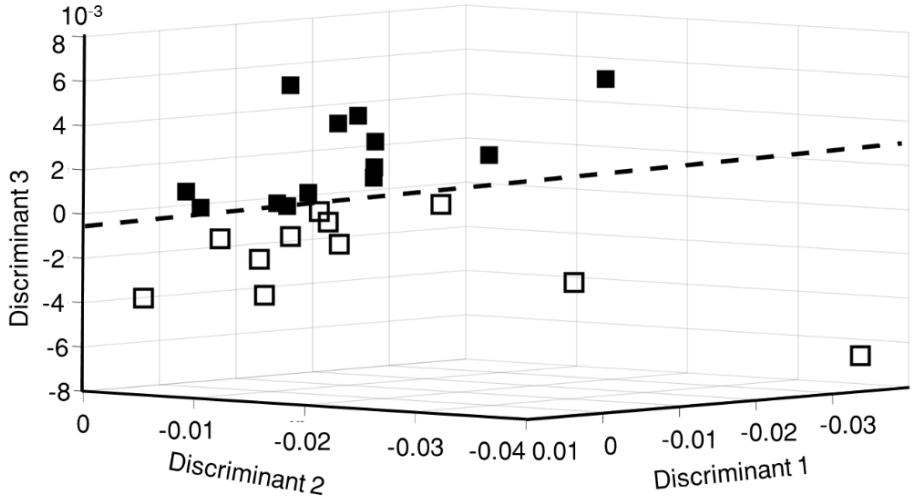

Figure 4.1. 1 LDA results for 26 clamp samples (14 hypo, filled squares, 11, non-hypo, unfilled squares) using a combination of 6 VOCs to develop the hypo signature. The model demonstrates perfect separation (AUC, specificity, sensitivity = 1). Dashed line is helpful to visualize cut-off discriminating hypo and non-hypo samples.

4.2 Characterization Results

FESEM, UV/VIS, and contact angle measurement were used to characterize the sensing material and evaluate the film uniformity, particle size, and hydrophobicity properties. These characteristic properties play an important role in sensor performance.

4.2.1 Field Emission Scanning Electron Microscope (FESEM) Analysis

A JSM-7800F FESEM (JEOL USA, Peabody, MA, USA) was used to evaluate the morphological properties of the PEI/f-GNPs. FESEM images of the polymer f-GNPs were taken at an accelerating voltage of 20 kV and a working distance of 5.0 mm. The bright spots of f-GNPs, scattered all over the interdigitated electrodes with uniform dark film of polymer indicates very uniform film achieved using drop casting of f-GNPs and spin coating polymer layer over it. The presenting results (shown in figure 4.2) shows the formation of a uniform composite of f- GNPs and polymer across the electrodes. The uniform layer is required to achieve higher sensitivity and selectivity.

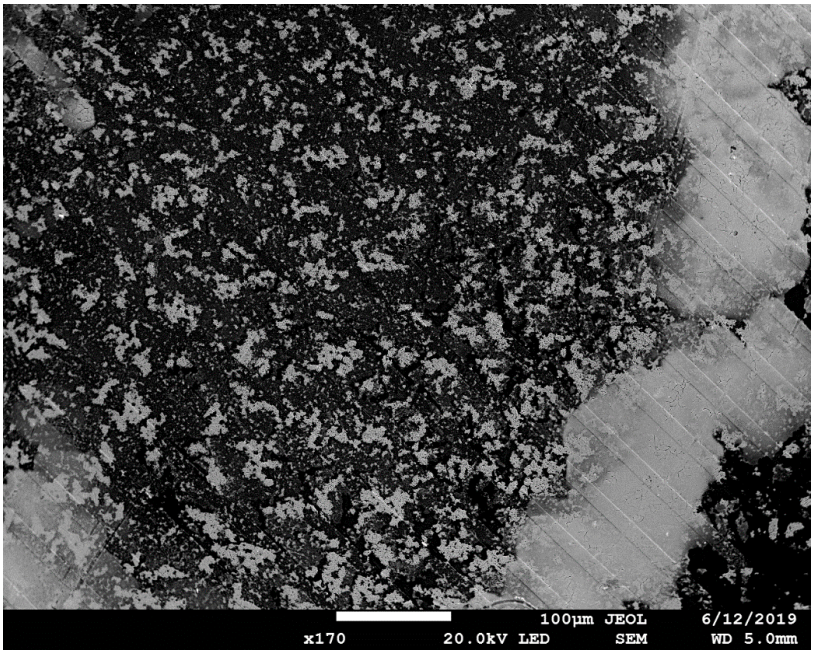

Figure 4.2. FESEM image of PEI-EGNP film showing EGNP particles embedded in polymer

Figure 4.3. A Raméhart Goniometer Model 200-F4 used for Contact Angle Measurement

4.2.2 Contact Angle Measurement

Raméhart contact angle goniometer model 200-F4 (Raméhart instrument co, Succasunna, NJ, USA) was to evaluate the wettability of the sensors via measuring the static contact angle between a water droplet and surface of the sensing film (instrument shown in the 4.3). The contact angle for all three sensors used in the sensor array is measured and presented in table 4.2. The comparison of contact angle in the three devices shows that PVDF-HFP-EGNP sensor presents the highest hydrophobicity and contanct angle of 94.6°. This leads to high stability toward water vapor. The contact angle of water droplet and PVDF-HFP/CB is measured to be 80.1°and smaller than PVDF-HFP-EGNP. This is due to addition of a glycerol (hydrophilic polymer) and treatment of the film with DEC. PEI-EGNP also shows a low hydrophilicity property and present a contact angle of 70°. The more hydrophobicity not only accounts for more stability under humid conditions, it also makes the sensors more sensitive and

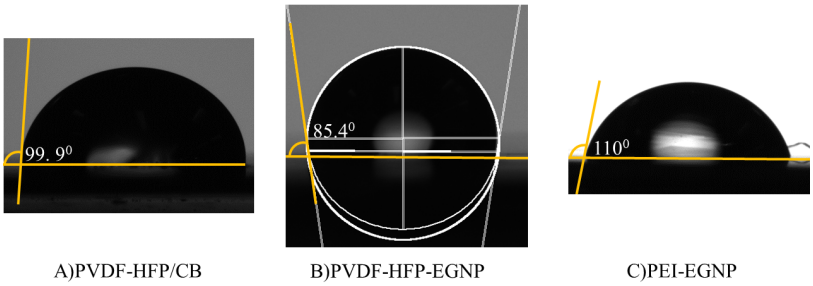

Figure 4.4. Contact Angle Measurements for Sensor Array A) PVDF-HFP/CB, B) PVDF-HFP-EGNP, and C) PEI-EGNP provided by software ImageJ

selective under humid conditions as the porous polymer only allows certain VOCs to interact with the conductive material and hence the sensors can be seen to have more sensitivity in humid conditions. The figure 4.4 (b) shows the contact angles given by the contact angle plugin on software ImageJ. The software measures the angle by fitting the water droplet to a circle or an ellipse, the values with circle fit (Theta C) are presented considering the materials. The software measures the inside angle that needs to be converted to contact angle.

Table 4.1. Contact Angle Measurements for Each Sensor Represented as Circle Fit (Theta C)

Sr. No	**Sensor Type**	**Theta C**
1	PVDF-HFP/CB	80.1°
2	PEI-EGNP	70°
3	PVDF-HFP-EGNP	94.6°

4.2.3 Ulta-Violet Visible (UV-VIS) Spectroscopy

UV-VIS measurement was conducted to evaluate the particle size and quality of the EGNPs used in this study. The light absorption is measured across the range of

300 nm to 700 nm and the results are shown in figure 4.5. The analysis suggests the surface plasmon resonance (SPR) peak is observed at a wavelength of 515 nm which indicates the spherical nanoparticles are smaller than 10 nm [156]. The analysis also indicates a ratio of 1.21 for SPR peak absorbance to the absorbance at 450 nm (ASPR / A450 nm)which estimates the size of EGNPs to be smaller than 5 nm [156]. This analysis is in agreement with the particle size reported by the company (3.5-5.5 nm).

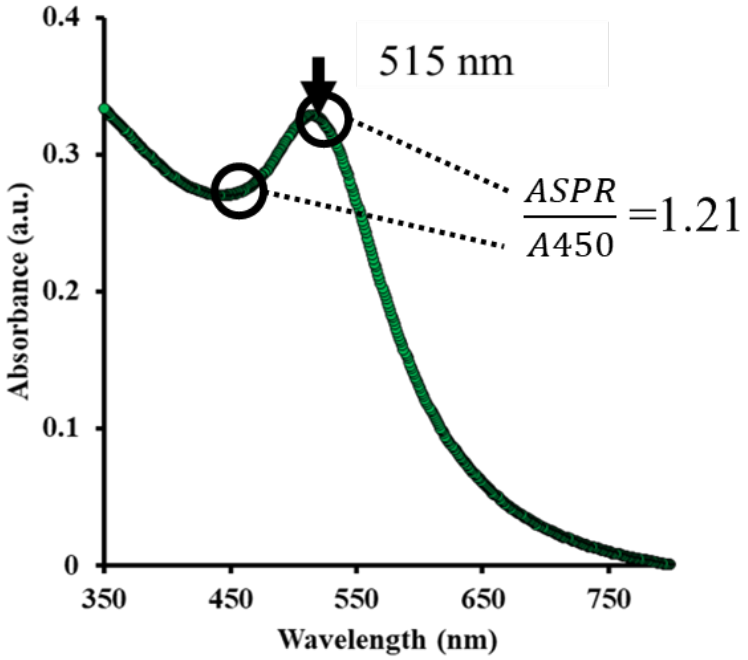

Figure 4.5. A UV-VIS analysis of EGNPs

4.3 Sensor Array Results

The sensors were tested with different VOCs at different concentrations and under different conditions. Four MFCs were utilized to expose the sensor to a specific flow of VOCs. Since the interaction of VOCs from blood with Exhaled breath happens at constant rate and concentration of these VOCs in the breath is affected by the va-

por pressure of the VOCs, instead of concentration, flow rate was used to determine the sensitivity of the sensor, especially under the simulated breath environment, To determine the specificity of the sensor, concentration was calculated using formula described in Chapter 3 (Section 3.3). The flow was measured in $SCCM$. The resistance was measured every 0.7 s but since multiple sensors were tested together each sensor response is 11.5-11.06 seconds apart. The fabricated sensors are shown in figure 4.6.

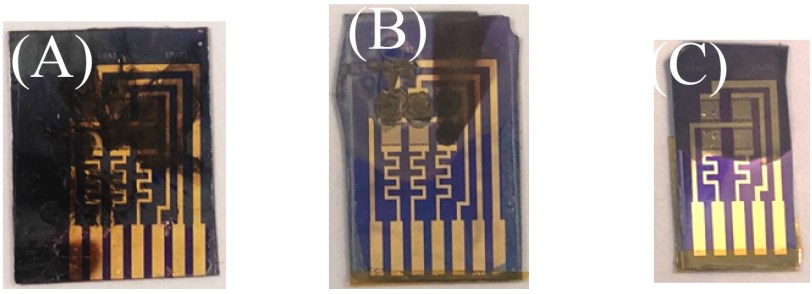

Figure 4.6. Contact Angle Measurements for Sensor Array A) PVDF-HFP/CB, B) PVDF-HFP-EGNP, and C) PEI-EGNP provided by software ImageJ

4.3.1 Sensor Array Response to Individual Targeting VOCs

The sensor array was tested with individual VOCs to test its sensitivity and selectivity. The sensor was stabilized at 400 $SCCM$ dry airflow for at least 30 minutes. The sensor was then exposed to 50 $SCCM$ of VOC for 3-cycles while keeping the total flow rate constant. Table 4.3 shows the calculated ppm concentration values. VOC3, VOC 4 and VOC 5 are the VOCs of interest as they have been seen in the breath data as potential biomarkers for hypoglycemia. All these VOCs are present in breath and have been identified as biomarkers for different diseases.

The sensor response to VOCs is summarized in Table 4.4. All the sensors in sensor array are most sensitive towards VOC4 since the concentration of the VOC is more due to its high vapor pressure. But figure 4.7 showing the comparison of sensor

Table 4.2. Targeting VOC and its Concentration in Parts per Million(ppm)

Name of VOC	**Concentration inside the testing chamber**
VOC1	163 ppm
VOC2	68 ppm
VOC3	37 ppm
VOC4	431 ppm
VOC5	34 ppm

response with respect to the VOCs, based on the calculation of response for 1ppm, indicates that sensors are more selective towards VOC5 and VOC3.

Table 4.3. Sensor Array Response to Targeting VOCs ($\%\Delta R/R_0$)

Name	**PVDF-HFP/CB**	**PEI-EGNP**	**PVDF-HFP-EGNP**
VOC1	0.212	0.718	3.978
VOC2	0.236	0.850	4.003
VOC3	0.190	0.568	3.029
VOC4	0.265	1.060	5.130
VOC5	0.193	0.712	3.926

4.3.2 Sensor Array Response to Multiple Targeting VOCs

The sensor array was tested with a combination of three VOCs to check its response to a VOC signature. Fig 4.7 shows a PCA analysis that separates this VOC signature from other signatures. The Panel that contains VOC3 and VOC5 have been separated from the cluster as shown by PCA. The PCA shows combination of VOC4 are clustered away from combinations of VOC1.. Here the PCA is looking at low re-

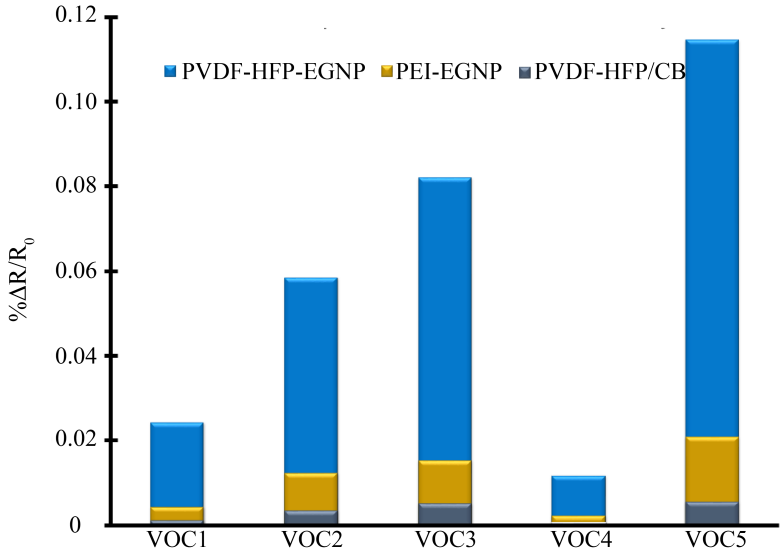

Figure 4.7. Sensor Response to Individual Targeting VOCs in Dry Air

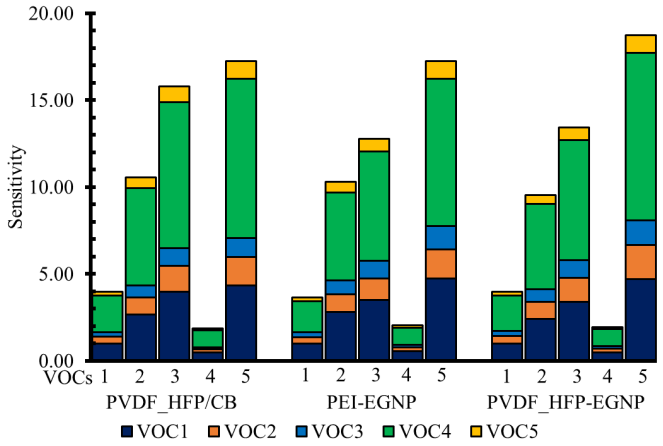

Figure 4.8. Sensor Selectivity Towards Each VOC with respect to other VOCs

sponse to combinations of VOC4. The figure 4.9 shows the PCA along the principle component 2 that shows that the desired panel of VOC1, VOC4, and VOC5 is separated from other panels while along the PC 3, the combination of VOC1, VOC3, and VOC5 is also separated from the other combinations. This shows the discriminating power of the proposed sensor array in detecting the signature of hypoglycemia which includes a combination of VOCs.

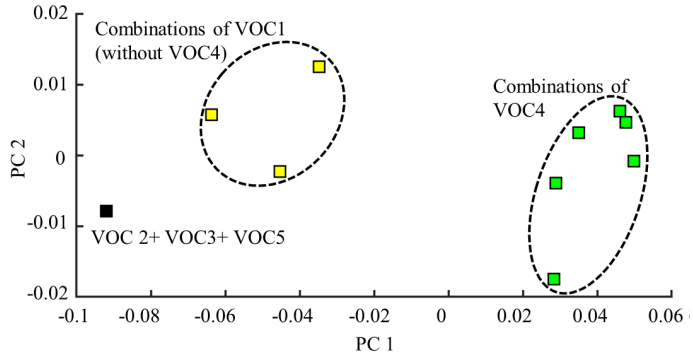

(a) PCA plot along first two principle components

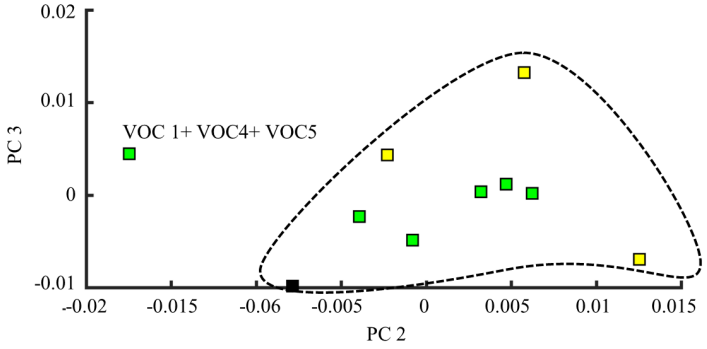

(b) PCA plot along second and third principle components

Figure 4.9. PCA Analysis of Percentage Resistance Change Showing Separation Between Multiple Signatures

4.3.3 Sensor Array Response to Simulated Breath

The sensor array was tested with simulated breath with and without VOC. The sensors response is evaluated similarly to the dry air. Fig. 4.8 shows a comparison between simulated breath and dry air response for the PEI-EGNP sensor. The response is more than 200% of the response to VOCs in dry air. The sensor becomes more sensitive in the presence of high humidity due to the interaction of water molecules with the polymer film. The average percentage response to all the VOCs is summa-

rized in Table 4.5. The three selected sensors detect three different VOCs selectively in the simulated breath. The PEI-EGNP detects VOC 4, PVDF-HFP-EGNP detects VOC1, while VOC5 is detected by PVDF-HFP/CB sensor. The enhanced sensitivity is observed due to the presence of high humidity that interacts with the polymer. The proposed sensing mechanism here is based on the observations. The polymer layer is protecting the EGNPs and also allowing the VOCs to interacting with EGNPs selectively.

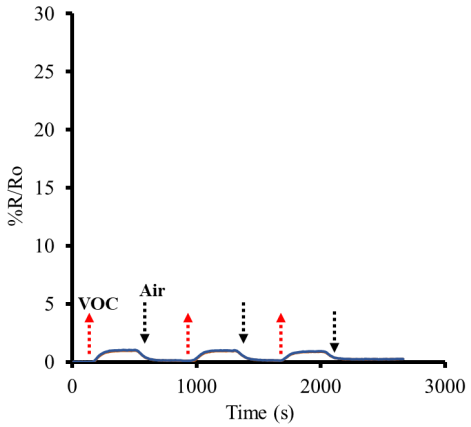

(a) Sensor Response in Dry Air

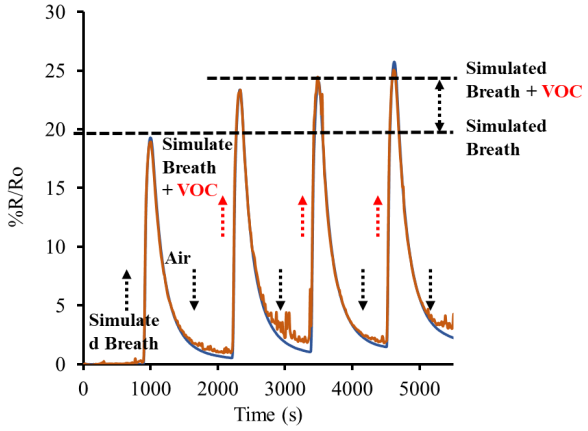

(b) Sensor Response in Simulated Breath

Figure 4.10. Comparison of Sensor Response to Individual VOC in Dry Air and Simulated Breath

Table 4.4. Sensor Array Response to Targeting VOCs in Simulated Breath ($\%\Delta R/R_0$)

Name	**PEI-EGNP**	**PVDF-HFP-EGNP**	**PVDF-HFP/CB**
VOC1	-0.280	**3.570**	-2.233
VOC2	1.241	1.383	0.590
VOC3	0.788	-1.554	0.554
VOC4	**3.896**	2.433	0.609
VOC5	2.981	2.049	**1.029**

4.3.4 Sensor Reproducibility Analysis

The sensors from sensor array were damaged during testing with the simulated breath due to prolonged exposure to humidity. The sensor was then placed in a vacuum to recover analyze the recovery and were tested after two days. PVDF-HFP-EGNP sensor was damaged and lost its sensitivity while the PEI-EGNP and PVDF-HFP/CB sensor were still equally sensitive. The PVDF-HFP-EGNP and PVDF-HFP/CB sensor were replaced to investigate reproducibility. Table 4.6 and Fig 4.9 shows the sensor array response before and after replacement. The sensor was tested with a single VOC for three cycles and the average sensor response is compared. 4.11 shows the average response of the old and new sensor array to VOC4 for three cycles, considering the response to the first array as 100%. Both sensors have been fabricated similarly but on different days. The presenting results show that change between the sensor responses of the two separate sets of sensors fabricated in a period of a week is less than 10%.

4.4 Sensor System Characterization and Results

The interface circuit consists of two signal conditioning circuits to accommodate two different types of sensors as described in methods. The circuit was first simulated

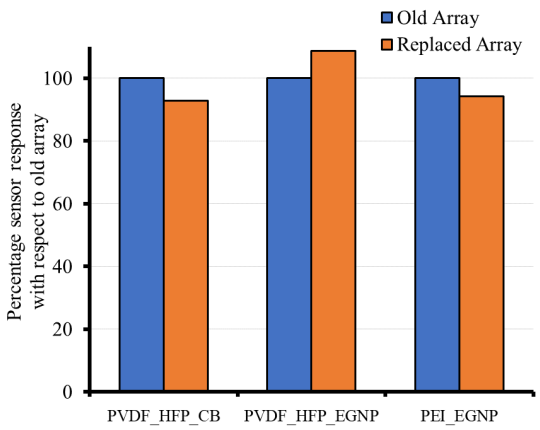

Figure 4.11. Sensor Response compared before and after replacement

Table 4.5. Reproducibility of Sensor Array Response to VOC4 ($\%\Delta R/R_0$)

	PEI-EGNP	**PVDF-HFP-EGNP**	**PVDF-HFP/CB**
Old Sensor	1.060	5.130	0.337
Replaced Sensor	1.000	5.582	0.313

on Pspice with $5V$ as input voltage and then was compared with experimental results for the same on the system. Fig 4.10 shows the circuit used for simulations. The system consists of two circuits to accommodate two different types of sensors, the values of the bridge resistors were optimized for linearity and gain in the working range of the sensor.

4.4.1 Comparison Between Experimental and Simulation Results

The interface circuit was fabricated and developed using the electronics presented in the material and method. The electrical system was powered by a 5V power supply from a PC USB port. The experimental results showed a drop of 500 mV in the voltage observed across the sensors. The output voltage change due to the change

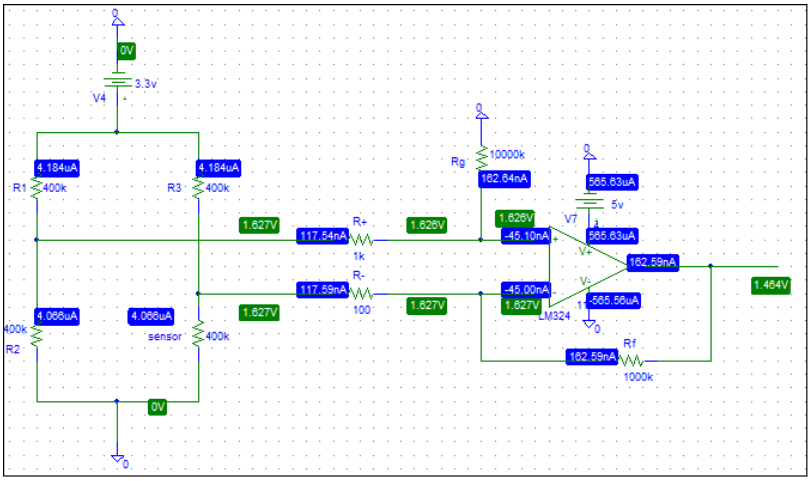

Figure 4.12. Simulation example of circuit on Pspice

to the sensor resistance was in agreement with the simulation results (shown in figure 4.13).

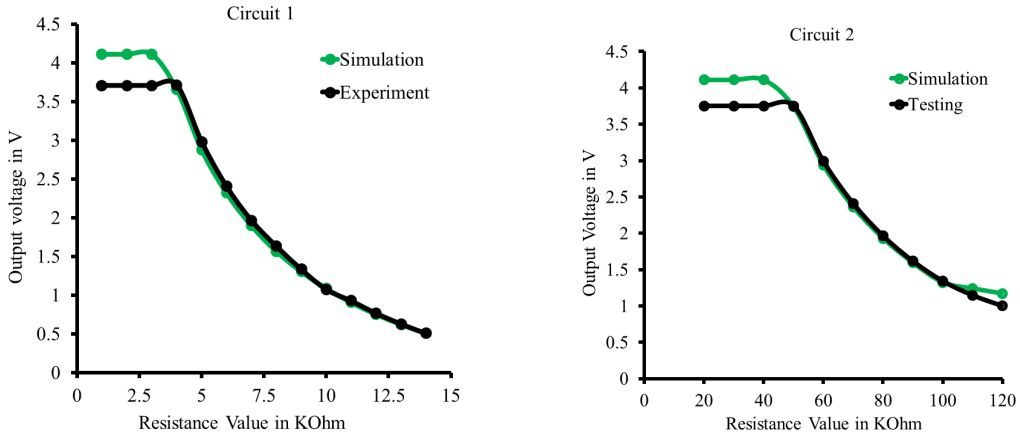

(a) Comparison for Circuit 1

(b) Comparison for Circuit 2

Figure 4.13. Comparison between simulation and experimental results

4.4.2 Impact of Power Supply :Open Circuit Voltage

The electrical system is designed to be used with different batteries. The performance of the electrical system in detecting resistance change of the sensor using power supplies with different batteries has been investigated and the results are shown in figure 4.14. The presenting results show that the sensors can correctly detect the resistance change of the sensors in a range of 50 $K\Omega$ to 120 $K\Omega$. This shows the engineered circuit can be used with a variety of power supplies in different applications. A version of a system was also tested with multiple power supply voltages to configure a portable battery and a power supply for the whole system. The Arduino requires min $5V$ supply when connected to a computer it draws sufficient voltage to function at maximum efficiency. Since the subparts of the system are connected to a $5V$ and $3.3V$ out pin from Arduino, the system response changes when power supply voltage changes. The experimental results were collected by testing the system with a computer. The system was further tested with a $3.7V$ battery, a $3.7V$ battery with step-up transformer, and two 3V cells connected in series. These options were selected considering the size of the system and using the small available battery with maximum capacity and output current. As expected, the systems initial output drops due to low voltage power supply. The stepped-up 5V supply performs as good as the $6V$ supply.

The sensor system has been through multiple iterations and revisions. The parts were replaced, the design was revised to make a compact and reliable system. The system evolution from a simple multipurpose breadboard to optimised PCB is shown in figure 4.15.

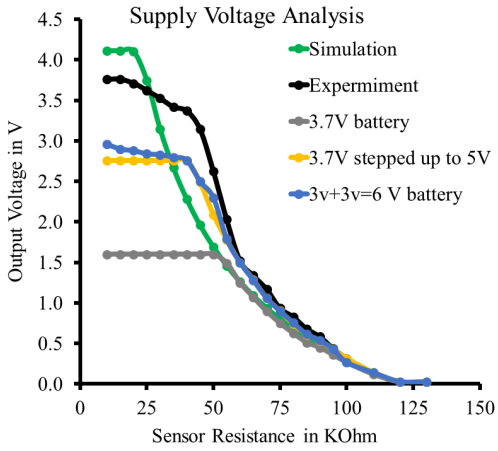

Figure 4.14. Simulation example of circuit on Pspice

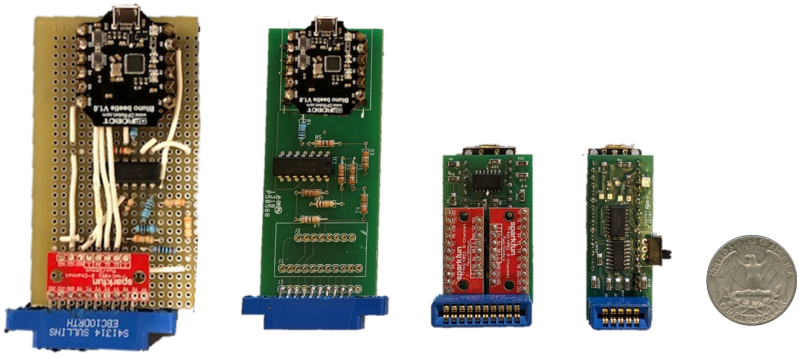

Figure 4.15. Evolution of Proposed Smart Sensor System

5. CONCLUSION AND FUTURE WORK

The Chapter describes the achievements of this thesis and proposes future work that can improve and enhance the proposed sensor system with advanced technology, fabrication, and testing methods to detect more VOCs and apply the system for breath analysis and other diseases detection.

5.1 Conclusion

The purpose of the project was to design and develop a portable system to detect a panel of VOCs related to hypoglycemia that has been seen before in diabetes breath samples by our research group and has been verified in the statistical analysis performed in the presented thesis. The chemiresistive sensors were developed using conductive polymer composite PVDF-HFP/CB and f-GNPs coated with polymer layer PEI and PVDF. The sensors were fabricated to detect VOCs in high humidity(greater than 90%) considering its application, the polymer layer helps in making the film more hydrophobic and the porous structure of the film allows the interaction of VOCs with sensing material. The PVDF-HFP/CB sensor was most hydrophobic and shows selectivity towards VOC5 and shows the least sensitivity towards the humidity of all proposed sensors due to high hydrophobicity. The PEI-EGNP sensor was selective towards VOC4 in simulated breath while the PVDF-HFP-EGNP sensor was most sensitive and was elective towards VOC1. The sensors were tested as an array to have cross selectivity and to detect the panel more accurately.

A smart sensor interface system was fabricated on PCB with BLE communication to allow connection of the system with a PDA to monitor and store data for the patients and doctors. An interface circuit has two unique signal conditioning circuits to accommodate multiple sensors. The circuit was simulated on Pspice with chang-

ing sensor resistance multiple times with different combinations of resistors for the Wheatstone bridge and amplification circuit to investigate the best possible combination, maximizing the range and gain of the circuit. The system was fabricated and tested with varying resistance to validate the simulation results. The system follows the simulation closely and can detect resistance change over the desired range for both the circuits. The system was also tested with multiple different power supplies to investigate its performance based on different power inputs. The system performance is maximum when the power supply is more than 5V and drops gradually as the power voltage drops. The system can be tuned to perform efficiently at low power voltage by updating the software. The system is controlled by an Arduino microcontroller that is programmed using Arduino software to perform control, data collection, and analysis on the sensors. The project will help improve the lives of millions of patients suffering from T1D or hypoglycemia by providing a noninvasive method to detect and predict hypoglycemia.

5.2 Future Work

The project can be advanced further in all three segments. More samples are currently been analyzed to validate the VOCs that can exclusively predict hypoglycemia on the breath sample, irrespective of the external factors like environment, age, gender, and other personal factors such as smoking or drinking. Fabricating multiple sensors on a single substrate can make the system compact and more portable. This will also enhance cross selectivity. These sensor arrays will need to be tested under the simulated condition with a combination of multiple VOCs to thoroughly understand the cross selectivity. The system can be miniaturized further to advanced by simply integrating interface circuits, Arduino, and BLE chip on the same PCB. This will also allow the arrangement of components at desired places and removal of redundant components from the off-the-shelf Arduino module. The system currently uses BLE for communication, a GSM module can be integrated into the system to communicate

with phones with no Bluetooth compatibility. This can further enhance the use of the device towards the people who do not have smart phones.A Wi-Fi module can also be included to send and receive alerts over Wi-Fi.

Currently, the prototype packaging that is designed in the project needs considerable modifications based on the breath analysis application. Though the sensors are not affected due to change in flow onto the sensors, a mouthpiece that can regulate the flow of exhaled breath onto the sensor is necessary to force the users to blow at a constant rate that will cause constant VOC exchange in lungs. A polymer layer on the inside walls of the packaging near the sensors or small chamber that can pre-concentrate the samples would help the sensors become more sensitive and accurate. The system can then be implemented in a clinical study to analyze the impact of using the system on diabetes management for patients with T1D. Reviews and feedbacks from the study will be useful in revising the system and also study system performance.

An app for data collection and data presentation is under development that can help the users to visualize the results in laymen terms. The app can also be programmed to store the data on the cloud and communicate with caregivers and doctors for support to the patient. The sensors and software can be modified to perform multiple analysis and detect different volatiles for different diseases. This way the system is customizable to the disease and other volatile detection applications due to its unique design.

REFERENCES

REFERENCES

[1] Emily Tu, Stephen M. Twigg, and Christopher Semsarian. Sudden death in type 1 diabetes: The mystery of the 'dead in bed' syndrome. *International Journal of Cardiology*, 138(1):91–93, January 2010.

[2] Philip J. Stout, Nina Peled, Brian J. Erickson, Michael E. Hilgers, Joel R. Racchini, and Thomas B. Hoegh. Comparison of Glucose Levels in Dermal Interstitial Fluid and Finger Capillary Blood, July 2004.

[3] Hua Deng, Lin Lin, Mizhi Ji, Shuangmei Zhang, Mingbo Yang, and Qiang Fu. Progress on the morphological control of conductive network in conductive polymer composites and the use as electroactive multifunctional materials. *Progress in Polymer Science*, 39(4):627–655, April 2014.

[4] Radu Ionescu, Umut Cindemir, Tesfalem Geremariam Welearegay, Raul Calavia, Zouhair Haddi, Zareh Topalian, Claes-Göran Granqvist, and Eduard Llobet. Fabrication of ultra-pure gold nanoparticles capped with dodecanethiol for Schottky-diode chemical gas sensing devices. *Sensors and Actuators B: Chemical*, 239:455–461, February 2017.

[5] Morad K. Nakhleh, Yoav Y. Broza, and Hossam Haick. Monolayer-capped gold nanoparticles for disease detection from breath. *Nanomedicine (London, England)*, 9(13):1991–2002, September 2014.

[6] Amanda P. Siegel, Ali Daneshkhah, Dana S. Hardin, Sudhir Shrestha, Kody Varahramyan, and Mangilal Agarwal. Analyzing breath samples of hypoglycemic events in type 1 diabetes patients: Towards developing an alternative to diabetes alert dogs. *Journal of breath research*, 11(2):026007, 2017.

[7] *Type 1 Diabetes Facts | JDRF*, 2019 (accessed November 5, 2019). https://www.jdrf.org/t1d-resources/about/facts/.

[8] *Type 1 Diabetes | American Diabetes Association*, 2019 (accessed June 14, 2019). http://www.diabetes.org/diabetes-basics/type-1/.

[9] *National Diabetes Statistics Report | Data & Statistics | Diabetes | CDC*, February 2019(accessed June 14, 2019). https://www.cdc.gov/diabetes/data/statistics-report/index.html.

[10] Diane Wild, Robyn von Maltzahn, Elaine Brohan, Torsten Christensen, Per Clauson, and Linda Gonder-Frederick. A critical review of the literature on fear of hypoglycemia in diabetes: Implications for diabetes management and patient education. *Patient Education and Counseling*, 68(1):10–15, September 2007.

[11] Kellee M. Miller, Nicole C. Foster, Roy W. Beck, Richard M. Bergenstal, Stephanie N. DuBose, Linda A. DiMeglio, David M. Maahs, and William V. Tamborlane. Current State of Type 1 Diabetes Treatment in the U.S.: Updated Data from the T1D Exchange Clinic Registry. *Diabetes Care*, 38(6):971–978, June 2015.

[12] Deborah L. Wells, Shaun W. Lawson, and A. Niroshan Siriwardena. Canine responses to hypoglycemia in patients with type 1 diabetes. *Journal of Alternative and Complementary Medicine (New York, N.Y.)*, 14(10):1235–1241, December 2008.

[13] Jennifer Cattet, Dana Hardin, Wes Anderson, and Zachary Shrivaneck. Hypoglycemia Alert Dogs: Innovative Assistance for People with Type 1 Diabetes. June 2013.

[14] Nicola J. Rooney, Steve Morant, and Claire Guest. Investigation into the value of trained glycaemia alert dogs to clients with type I diabetes. *PloS One*, 8(8):e69921, 2013.

[15] Linda Gonder-Frederick, Pam Rice, Dan Warren, Karen Vajda, and Jaclyn Shepard. Diabetic alert dogs: A preliminary survey of current users. *Diabetes Care*, 36(4):e47, April 2013.

[16] M. Chen, M. Daly, N. Williams, S. Williams, C. Williams, and G. Williams. Non-invasive detection of hypoglycaemia using a novel, fully biocompatible and patient friendly alarm system. *BMJ (Clinical research ed.)*, 321(7276):1565–1566, December 2000.

[17] N. M. Petry, J. A. Wagner, C. J. Rash, and K. K. Hood. Perceptions about professionally and non-professionally trained hypoglycemia detection dogs. *Diabetes Research and Clinical Practice*, 109(2):389–396, August 2015.

[18] Tadeusz Jezierski, Marta Walczak, Tomasz Ligor, Joanna Rudnicka, and Bogusław Buszewski. Study of the art: Canine olfaction used for cancer detection on the basis of breath odour. Perspectives and limitations. *Journal of Breath Research*, 9(2):027001, May 2015.

[19] Nicolas Goossens, Shigeki Nakagawa, Xiaochen Sun, and Yujin Hoshida. Cancer biomarker discovery and validation. *Translational Cancer Research*, 4(3):256–269, June 2015.

[20] World Health Organization and International Programme on Chemical Safety. *Biomarkers in Risk Assessment : Validity and Validation*. World Health Organization, 2001.

[21] Christine M. Micheel, Sharly J. Nass, Gilbert S. Omenn, Committee on the Review of Omics-Based Tests for Predicting Patient Outcomes in Clinical Trials, Board on Health Care Services, Board on Health Sciences Policy, and Institute of Medicine. *Committee On The Review of Omics-Based Tests for Predicting Patient Outcomes in Clinical Trials*. National Academies Press (US), March 2012.

[22] Meggie Hakim, Yoav Y. Broza, Orna Barash, Nir Peled, Michael Phillips, Anton Amann, and Hossam Haick. Volatile Organic Compounds of Lung Cancer and Possible Biochemical Pathways. *Chemical Reviews*, 112(11):5949–5966, November 2012.

[23] Yoav Y. Broza and Hossam Haick. Nanomaterial-based sensors for detection of disease by volatile organic compounds. *Nanomedicine (London, England)*, 8(5):785–806, May 2013.

[24] Michael Phillips, Renee N. Cataneo, Christobel Saunders, Peter Hope, Peter Schmitt, and James Wai. Volatile biomarkers in the breath of women with breast cancer. *Journal of Breath Research*, 4(2):026003, June 2010.

[25] G. Peng, M. Hakim, Y. Y. Broza, S. Billan, R. Abdah-Bortnyak, A. Kuten, U. Tisch, and H. Haick. Detection of lung, breast, colorectal, and prostate cancers from exhaled breath using a single array of nanosensors. *British Journal of Cancer*, 103(4):542–551, August 2010.

[26] Ulrike Tisch, Ilana Schlesinger, Radu Ionescu, Maria Nassar, Noa Axelrod, Dorina Robertman, Yael Tessler, Faris Azar, Abraham Marmur, Judith Aharon-Peretz, and Hossam Haick. Detection of Alzheimer's and Parkinson's disease from exhaled breath using nanomaterial-based sensors. *Nanomedicine (London, England)*, 8(1):43–56, January 2013.

[27] B. J. Novak, D. R. Blake, S. Meinardi, F. S. Rowland, A. Pontello, D. M. Cooper, and P. R. Galassetti. Exhaled methyl nitrate as a noninvasive marker of hyperglycemia in type 1 diabetes. *Proceedings of the National Academy of Sciences of the United States of America*, 104(40):15613–15618, October 2007.

[28] Pietro R. Galassetti, Brian Novak, Dan Nemet, Christie Rose-Gottron, Dan M. Cooper, Simone Meinardi, Robert Newcomb, Frank Zaldivar, and Donald R. Blake. Breath ethanol and acetone as indicators of serum glucose levels: An initial report. *Diabetes Technology & Therapeutics*, 7(1):115–123, February 2005.

[29] Claire Turner, Christopher Walton, Shu Hoashi, and Mark Evans. Breath acetone concentration decreases with blood glucose concentration in type I diabetes mellitus patients during hypoglycaemic clamps. *Journal of Breath Research*, 3(4):046004, December 2009.

[30] Sankalpa Neupane, Robert Peverall, Graham Richmond, Tom P. J. Blaikie, David Taylor, Gus Hancock, and Mark L. Evans. Exhaled Breath Isoprene Rises During Hypoglycemia in Type 1 Diabetes. *Diabetes Care*, 39(7):e97–e98, July 2016.

[31] Tom P. J. Blaikie, Julie A. Edge, Gus Hancock, Daniel Lunn, Clare Megson, Rob Peverall, Graham Richmond, Grant A. D. Ritchie, and David Taylor. Comparison of breath gases, including acetone, with blood glucose and blood ketones in children and adolescents with type 1 diabetes. *Journal of Breath Research*, 8(4):046010, November 2014.

[32] Susanne Halbritter, Mattia Fedrigo, Vera Höllriegl, Wilfried Szymczak, Joerg M. Maier, Anette-Gabriele Ziegler, and Michael Hummel. Human Breath Gas Analysis in the Screening of Gestational Diabetes Mellitus. *Diabetes Technology & Therapeutics*, 14(10):917–925, October 2012.

[33] Timothy D. C. Minh, Stacy R. Oliver, Jerry Ngo, Rebecca Flores, Jason Midyett, Simone Meinardi, Matthew K. Carlson, F. Sherwood Rowland, Donald R. Blake, and Pietro R. Galassetti. Noninvasive measurement of plasma

glucose from exhaled breath in healthy and type 1 diabetic subjects. *American Journal of Physiology. Endocrinology and Metabolism*, 300(6):E1166–1175, June 2011.

[34] Liam M. Heaney and Martin R. Lindley. Translation of exhaled breath volatile analyses to sport and exercise applications. *Metabolomics*, 13(11):139, 2017.

[35] Harshada Patil, Vani Sane, Sriram G, Indumathi T.s, and Preeta Sharan. Gallium arsenide based surface plasmon tesonance for glucose monitoring. In *International Conference on Optical and Photonic Engineering (icOPEN 2015)*, volume 9524, page 95242E. International Society for Optics and Photonics, July 2015.

[36] *Diabetic Alert Dogs of America (dadofamerica)*, 2019 (accessed June 14, 2019). https://www.diabeticalertdogsofamerica.com.

[37] *Penn Vet | Diabetes Program*, 2019 (accessed June 14, 2019). https://www.vet.upenn.edu/veterinary-hospitals/ryan-veterinary-hospital/services/internal-medicine/diabetes-program.

[38] Dana S. Hardin, Wesley Anderson, and Jennifer Cattet. Dogs Can Be Successfully Trained to Alert to Hypoglycemia Samples from Patients with Type 1 Diabetes. *Diabetes Therapy*, 6(4):509–517, December 2015.

[39] K. H. Kim, Shamin Ara Jahan, and Ehsanul Kabir. A review of breath analysis for diagnosis of human health. *TrAC Trends in Analytical Chemistry*, 33:1–8, March 2012.

[40] Konstantinos A. Kouremenos, Mikael Johansson, and Philip J. Marriott. Advances in Gas Chromatographic Methods for the Identification of Biomarkers in Cancer. *Journal of Cancer*, 3:404–420, September 2012.

[41] K. Namjou, C. B. Roller, and G. McMillen. Breath-Analysis Using Mid-Infrared Tunable Laser Spectroscopy. In *2007 IEEE SENSORS*, pages 1337–1340, October 2007.

[42] L. R. Narasimhan, William Goodman, and C. Kumar N. Patel. Correlation of breath ammonia with blood urea nitrogen and creatinine during hemodialysis. *Proceedings of the National Academy of Sciences*, 98(8):4617–4621, April 2001.

[43] Susan E Ebeler, Andrew J Clifford, and Takayuki Shibamoto. Quantitative analysis by gas chromatography of volatile carbonyl compounds in expired air from mice and human. *Journal of Chromatography B: Biomedical Sciences and Applications*, 702(1):211–215, November 1997.

[44] Andreas Wehinger, Alex Schmid, Sergei Mechtcheriakov, Maximilian Ledochowski, Christoph Grabmer, Guenther A. Gastl, and Anton Amann. Lung cancer detection by proton transfer reaction mass-spectrometric analysis of human breath gas. *International Journal of Mass Spectrometry*, 265(1):49–59, August 2007.

[45] David Smith and Patrik Španěl. Ambient analysis of trace compounds in gaseous media by SIFT-MS. *Analyst*, 136(10):2009–2032, April 2011.

[46] Progress in SIFT-MS: Breath analysis and other applications. *Mass Spectrometry Reviews*, 30(2):236–267, March 2011.

[47] David Smith, Tianshu Wang, Josep Sulé-Suso, Patrik Španěl, and Alicia El Haj. Quantification of acetaldehyde released by lung cancer cells in vitro using selected ion flow ttube mass spectrometry. *Rapid Communications in Mass Spectrometry*, 17(8):845–850, 2003.

[48] Patrik Španěl, Simon Davies, and David Smith. Quantification of breath isoprene using the selected ion flow tube mass spectrometric analytical method. *Rapid Communications in Mass Spectrometry*, 13(17):1733–1738, 1999.

[49] Gas Chromatography and Mass Spectrometry: A Practical Guide - 2nd Edition.

[50] Sandra Van den Velde, Frederik Nevens, Paul Van hee, Daniel van Steenberghe, and Marc Quirynen. GC–MS analysis of breath odor compounds in liver patients. *Journal of Chromatography B*, 875(2):344–348, November 2008.

[51] T Ligor, M Ligor, A Amann, C Ager, M Bachler, A Dzien, and B Buszewski. The analysis of healthy volunteers' exhaled breath by the use of solid-phase mcroextraction and GC-MS. *Journal of Breath Research*, 2(4):046006, December 2008.

[52] A. Bajtarevic, C. Ager, M. Pienz, M. Klieber, K. Schwarz, M. Ligor, T. Ligor, W. Filipiak, H. Denz, M. Fiegl, W. Hilbe, W. Weiss, P. Lukas, H. Jamnig, M. Hackl, A. Haidenberger, B. Buszewski, W. Miekisch, J. Schubert, and A. Amann. Noninvasive detection of lung cancer by analysis of exhaled breath. *BMC Cancer*, 9:348, 2009.

[53] Diana Poli, Matteo Goldoni, Massimo Corradi, Olga Acampa, Paolo Carbognani, Eveline Internullo, Angelo Casalini, and Antonio Mutti. Determination of aldehydes in exhaled breath of patients with lung cancer by means of on-fiber-derivatisation SPME–GC/MS. *Journal of Chromatography B*, 878(27):2643–2651, October 2010.

[54] Jane Lee, Jerry Ngo, Don Blake, Simone Meinardi, Andria M. Pontello, Robert Newcomb, and Pietro R. Galassetti. Improved predictive models for plasma glucose estimation from multi-linear regression analysis of exhaled volatile organic compounds. *Journal of Applied Physiology*, 107(1):155–160, July 2009.

[55] Mark Woollam, Meghana Teli, Paula Angarita-Rivera, Shengzhi Liu, Amanda P. Siegel, Hiroki Yokota, and Mangilal Agarwal. Detection of Volatile Organic Compounds (VOCs) in Urine via Gas Chromatography-Mass Spectrometry QTOF to Differentiate Between Localized and Metastatic Models of Breast Cancer. *Scientific Reports*, 9(1):1–12, February 2019. Number: 1 Publisher: Nature Publishing Group.

[56] Alphus Dan Wilson. Review of Electronic-nose Technologies and Algorithms to Detect Hazardous Chemicals in the Environment. *Procedia Technology*, 1:453–463, January 2012.

[57] Mark Modrak, Victor D'Amato, Michiel Doorn, Ram Hashmonay, Walter Vergara, Alejandro Deeb, Carlos Suarez, and Carlos Aparicio. Characterization of Fugitive Emissions of Greenhouse Gases from a Wastewater Treatment Plant

Using the Radial Plume Mapping Technique. *Proceedings of the Water Environment Federation*, 2006(5):7200–7205, January 2006.

[58] Gary A. Eiceman, Jorge Gardea-Torresdey, Frank Dorman, Ed Overton, A. Bhushan, and H. P. Dharmasena. Gas Chromatography. *Analytical Chemistry*, 78(12):3985–3996, June 2006.

[59] S. Fuchs, P. Strobel, M. Siadat, and M. Lumbreras. Evaluation of unpleasant odor with a portable electronic nose. *Materials Science and Engineering: C*, 28(5):949–953, July 2008.

[60] Jacques Nicolas, Anne-Claude Romain, and Catherine Ledent. The electronic nose as a warning device of the odour emergence in a compost hall. *Sensors and Actuators B: Chemical*, 116(1):95–99, July 2006.

[61] E Comini, G Faglia, G Sberveglieri, Y. X Li, W Wlodarski, and M. K Ghantasala. Sensitivity enhancement towards ethanol and methanol of tio_2 films doped with Pt and Nb. *Sensors and Actuators B: Chemical*, 64(1):169–174, June 2000.

[62] M. Giordano, M. Russo, A. Cusano, and G. Mensitieri. An high sensitivity optical sensor for chloroform vapours detection based on nanometric film of -form syndiotactic polystyrene. *Sensors and Actuators B: Chemical*, 107(1):140–147, May 2005.

[63] Eric S. Tillman and Nathan S. Lewis. Mechanism of enhanced sensitivity of linear poly(ethylenimine)-carbon black composite detectors to carboxylic acid vapors. *Sensors and Actuators B: Chemical*, 96(1):329–342, November 2003.

[64] Ting Gao, Eric S. Tillman, and Nathan S. Lewis. Detection and Classification of Volatile Organic Amines and Carboxylic Acids Using Arrays of Carbon Black-Dendrimer Composite Vapor Detectors. *Chemistry of Materials*, 17(11):2904–2911, May 2005.

[65] Thichamporn Eaidkong, Radeemada Mungkarndee, Chaiwat Phollookin, Gamonwarn Tumcharern, Mongkol Sukwattanasinitt, and Sumrit Wacharasindhu. Polydiacetylene paper-based colorimetric sensor array for vapor phase detection and identification of volatile organic compounds. *Journal of Materials Chemistry*, 22(13):5970–5977, March 2012.

[66] Hengwei Lin, Minseok Jang, and Kenneth S. Suslick. Preoxidation for Colorimetric Sensor Array Detection of VOCs. *Journal of the American Chemical Society*, 133(42):16786–16789, October 2011.

[67] J. Lee, S. Lee, H. Jeong, S. Lim, E. Jang, N. Yoon, D. Kwon, and S. Kang. Volatile organic compounds optical fiber gas sensor based on evanescentl field coupling and solvatochromism. In *2013 IEEE SENSORS*, pages 1–4, November 2013.

[68] Henry. Wohltjen and Raymond. Dessy. Surface acoustic wave probe for chemical analysis. I. Introduction and instrument description. *Analytical Chemistry*, 51(9):1458–1464, August 1979.

[69] Cristian Viespe and Constantin Grigoriu. Surface acoustic wave sensors with carbon nanotubes and SiO_2/Si nanoparticles based nanocomposites for VOC detection. *Sensors and Actuators B: Chemical*, 147(1):43–47, May 2010.

[70] Cristian Viespe and Dana Miu. Characteristics of Surface Acoustic Wave Sensors with Nanoparticles Embedded in Polymer Sensitive Layers for VOC Detection. *Sensors (Basel, Switzerland)*, 18(7), July 2018.

[71] R. T. Howe and R. S. Muller. Resonant-microbridge vapor sensor. *IEEE Transactions on Electron Devices*, 33(4):499–506, April 1986.

[72] Xiao Fan and Binyang Du. Selective detection of trace p-xylene by polymer-coated QCM sensors. *Sensors and Actuators B: Chemical*, 166-167:753–760, May 2012.

[73] Arnaldo D'Amico, Giorgio Pennazza, Marco Santonico, Eugenio Martinelli, Claudio Roscioni, Giovanni Galluccio, Roberto Paolesse, and Corrado Di Natale. An investigation on electronic nose diagnosis of lung cancer. *Lung Cancer (Amsterdam, Netherlands)*, 68(2):170–176, May 2010.

[74] Corrado Di Natale, Antonella Macagnano, Eugenio Martinelli, Roberto Paolesse, Giuseppe D'Arcangelo, Claudio Roscioni, Alessandro Finazzi-Agrò, and Arnaldo D'Amico. Lung cancer identification by the analysis of breath by means of an array of non-selective gas sensors. *Biosensors and Bioelectronics*, 18(10):1209–1218, September 2003.

[75] G. S. Wilson, Y. Zhang, G. Reach, D. Moatti-Sirat, V. Poitout, D. R. Thévenot, F. Lemonnier, and J. C. Klein. Progress toward the development of an implantable sensor for glucose. *Clinical Chemistry*, 38(9):1613–1617, September 1992.

[76] Jiri. Janata and Andras. Bezegh. Chemical sensors. *Analytical Chemistry*, 60(12):62–74, June 1988.

[77] Bartosz Szulczyński and Jacek Gebicki. Currently Commercially Available Chemical Sensors Employed for Detection of Volatile Organic Compounds in Outdoor and Indoor Air. *Environments*, 4(1):21, March 2017.

[78] S. Mendis, P.A. Sobotka, and D.E. Euler. Pentane and isoprene in expired air from humans: Gas-chromatographic analysis of single breath. *Clinical Chemistry*, 40(8):1485–1488, 1994.

[79] M. Folke, L. Cernerud, M. Ekström, and B. Hök. Critical review of non-invasive respiratory monitoring in medical care. *Medical and Biological Engineering and Computing*, 41(4):377–383, July 2003.

[80] Christopher O. Olopade, James A. Christon, Mohamed Zakkar, William I. Swedler, Israel Rubinstein, Chi-wei Hua, and Peter A. Scheff. Exhaled Pentane and Nitric Oxide Levels in Patients with Obstructive Sleep Apnea. *Chest*, 111(6):1500–1504, June 1997.

[81] Paolo Paredi, Sergei A. Kharitonov, and Peter J. Barnes. Elevation of Exhaled Ethane Concentration in Asthma. *American Journal of Respiratory and Critical Care Medicine*, 162(4):1450–1454, October 2000.

[82] Paolo Paredi, Sergei A. Kharitonov, David Leak, Simon Ward, David Cramer, and Peter J. Barnes. Exhaled Ethane, a Marker of Lipid Peroxidation, is Elevated in Chronic Obstructive Pulmonary Disease. *American Journal of Respiratory and Critical Care Medicine*, 162(2):369–373, August 2000.

[83] Jacek Gebicki and Adam Kloskowski. Electrochemical Sensor for Measurement of Volatile Organic Compounds Employing Square Wave Perturbation Voltage. *Metrology and Measurement Systems*, 17(4):637–649, January 2010.

[84] Ali Daneshkhah, Sudhir Shrestha, Mangilal Agarwal, and Kody Varahramyan. Poly(vinylidene fluoride-hexafluoropropylene) composite sensors for volatile organic compounds detection in breath. *Sensors and Actuators B: Chemical*, 221:635–643, December 2015.

[85] A. Daneshkhah, S. Shrestha, M. Agarwal, and K. Varahramyan. PPy/PMMA/PEG-based sensor for low-concentration acetone detection. In *Smart Biomedical and Physiological Sensor Technology XI*, volume 9107, page 910712. International Society for Optics and Photonics, May 2014.

[86] Ali Daneshkhah, Sudhir Shrestha, Amanda Siegel, Kody Varahramyan, and Mangilal Agarwal. Cross-Selectivity Enhancement of Poly(vinylidene fluoride-hexafluoropropylene)-Based Sensor Arrays for Detecting Acetone and Ethanol. *Sensors*, 17(3):595, March 2017.

[87] Ali Daneshkhah, Shitiz Vij, Amanda P. Siegel, and Mangilal Agarwal. Polyetherimide/carbon black composite sensors demonstrate selective detection of medium-chain aldehydes including nonanal. *Chemical Engineering Journal*, page 123104, October 2019.

[88] M. Leidinger, T. Sauerwald, T. Conrad, W. Reimringer, G. Ventura, and A. Schütze. Selective Detection of Hazardous Indoor VOCs Using Metal Oxide Gas Sensors. *Procedia Engineering*, 87:1449–1452, 2014.

[89] M. Schüler, N. Helwig, A. Schütze, T. Sauerwald, and G. Ventura. Detecting trace-level concentrations of volatile organic compounds with metal oxide gas sensors. In *2013 IEEE SENSORS*, pages 1–4, November 2013.

[90] Surajit Some, Yang Xu, Youngmin Kim, Yeoheung Yoon, Hongyi Qin, Atul Kulkarni, Taesung Kim, and Hyoyoung Lee. Highly Sensitive and Selective Gas Sensor Using Hydrophilic and Hydrophobic Graphenes. *Scientific Reports*, 3:1868, June 2013.

[91] Ganhua Lu, Leonidas E. Ocola, and Junhong Chen. Reduced graphene oxide for room-temperature gas sensors. *Nanotechnology*, 20(44):445502, October 2009.

[92] Jaehyun Chung, Kyong-Hoon Lee, Junghoon Lee, Diego Troya, and George C. Schatz. Multi-walled carbon nanotubes experiencing electrical breakdown as gas sensors. *Nanotechnology*, 15(11):1596–1602, October 2004.

[93] O. K. Varghese, P. D. Kichambre, D. Gong, K. G. Ong, E. C. Dickey, and C. A. Grimes. Gas sensing characteristics of multi-wall carbon nanotubes. *Sensors and Actuators B: Chemical*, 81(1):32–41, December 2001.

[94] S. Chatterjee, M. Castro, and J. F. Feller. An e-nose made of carbon nanotube based quantum resistive sensors for the detection of eighteen polar/nonpolar VOC biomarkers of lung cancer. *Journal of Materials Chemistry B*, 1(36):4563–4575, 2013.

[95] Yael Zilberman, Ulrike Tisch, Gregory Shuster, Wojciech Pisula, Xinliang Feng, Klaus Müllen, and Hossam Haick. Carbon Nanotube/Hexa-perihexabenzocoronene Bilayers for Discrimination Between Nonpolar Volatile Organic Compounds of Cancer and Humid Atmospheres. *Advanced Materials*, 22(38):4317–4320, 2010.

[96] Gang Peng, Elena Trock, and Hossam Haick. Detecting Simulated Patterns of Lung Cancer Biomarkers by Random Network of Single-Walled Carbon Nanotubes Coated with Nonpolymeric Organic Materials. *Nano Letters*, 8(11):3631–3635, November 2008.

[97] Hank Wohltjen and Arthur W. Snow. Colloidal MetalInsulatorMetal Ensemble Chemiresistor Sensor. *Analytical Chemistry*, 70(14):2856–2859, July 1998.

[98] Jay W. Grate, David A. Nelson, and Rhonda Skaggs. Sorptive Behavior of Monolayer-Protected Gold Nanoparticle Films: Implications for Chemical Vapor Sensing. *Analytical Chemistry*, 75(8):1868–1879, April 2003.

[99] Ekaterina Dovgolevsky, Ulrike Tisch, and Hossam Haick. Chemically Sensitive Resistors Based on Monolayer-Capped Cubic Nanoparticles: Towards Configurable Nanoporous Sensors. *Small*, 5(10):1158–1161, 2009.

[100] Arthur W. Snow, Mario G. Ancona, and Doewon Park. Nanodimensionally Driven Analyte Response Reversal in Gold Nanocluster Chemiresistor Sensing. *Langmuir*, 28(44):15438–15443, November 2012.

[101] Yvonne Joseph, Isabelle Besnard, Miriam Rosenberger, Berit Guse, Heinz-Georg Nothofer, Jurina M. Wessels, Ute Wild, Axel Knop-Gericke, Dangsheng Su, Robert Schlögl, Akio Yasuda, and Tobias Vossmeyer. Self-Assembled Gold Nanoparticle/Alkanedithiol Films: Preparation, Electron Microscopy, XPS-Analysis, Charge Transport, and Vapor-Sensing Properties. *The Journal of Physical Chemistry B*, 107(30):7406–7413, July 2003.

[102] Yang Jiang, Ning Tang, Cheng Zhou, Ziyu Han, Hemi Qu, and Xuexin Duan. A chemiresistive sensor array from conductive polymer nanowires fabricated by nanoscale soft lithography. *Nanoscale*, 10(44):20578–20586, November 2018.

[103] Boris Lakard, Stéphanie Carquigny, Olivier Segut, Tilia Patois, and Sophie Lakard. Gas Sensors Based on Electrodeposited Polymers. *Metals*, 5(3):1371–1386, September 2015.

[104] Yilong Li, Petra Pötschke, Jürgen Pionteck, and Brigitte Voit. Electrical and vapor sensing behaviors of polycarbonate composites containing hybrid carbon fillers. *European Polymer Journal*, 108:461–471, November 2018.

[105] Z. C. Kennedy, J. F. Christ, K. A. Evans, B. W. Arey, L. E. Sweet, M. G. Warner, R. L. Erikson, and C. A. Barrett. 3D-printed poly(vinylidene fluoride)/carbon nanotube composites as a tunable, low-cost chemical vapour sensing platform. *Nanoscale*, 9(17):5458–5466, May 2017.

[106] Selectivity of organic nanocomposite sensor for detection of aldehydes. pages 1–6, December 2013.

[107] A. N. Mallya and P. C. Ramamurthy. Organic Molecule Based Sensor for Aldehyde Detection. In Alex Mason, Subhas Chandra Mukhopadhyay, and Krishanthi Padmarani Jayasundera, editors, *Sensing Technology: Current Status and Future Trends III*, Smart Sensors, Measurement and Instrumentation, pages 299–325. Springer International Publishing, Cham, 2015.

[108] Rosana Alberici, Regina Sparrapan, Marcos N. Eberlin, Dario Windmöller, and Rodinei Augusti. Polyetherimide–silicone: A 10 µm ultrathin composite membrane for faster and more sensitive membrane introduction mass spectrometry analysis. *Analytical Communications*, 36(6):221–223, 1999.

[109] S. Deng, T. Liu, S. Sourirajan, and T. Matsuura. A Study of Volatile Hydrocarbon Emission Control by Polyetherimide Hollow Fiber Membranes. *Journal of Polymer Engineering*, 14(4):219–236, 2011.

[110] Dongliang Wang, K. Li, and W. K. Teo. Preparation and characterization of polyetherimide asymmetric hollow fiber membranes for gas separation. *Journal of Membrane Science*, 138(2):193–201, January 1998.

[111] Wei Zhao and Baoli Shi. Removal of Volatile Organic Compounds from Water by Pervaporation Using Polyetherimide-Polyethersulfone Blend Hollow Fiber Membranes. *Separation Science and Technology*, 44(8):1737–1752, June 2009.

[112] S. Deng, A. Tremblay, and T. Matsuura. Preparation of hollow fibers for the removal of volatile organic compounds from air. *Journal of Applied Polymer Science*, 69(2):371–379, 1998.

[113] Chih-Tsung Shih, Tsung-Min Huang, Chung-Ju Lee, Shinn-Sheng Yu, Jeng-Horng Chen, and Anthony Yen. Method of semiconductor integrated circuit fabrication, February 2016.

[114] Che-Wei Hsu, Fang-Ci Su, Po-Yu Peng, Hong-Tsu Young, Stephen Liao, and Gou-Jen Wang. Highly sensitive non-enzymatic electrochemical glucose biosensor using a photolithography fabricated micro/nano hybrid structured electrode. *Sensors and Actuators B: Chemical*, 230:559–565, July 2016.

[115] Kazuki Kasahara, Hong Xu, Vasiliki Kosma, Jeremy Odent, Emmanuel P. Giannelis, and Christopher K. Ober. Nanoparticle photoresist studies for EUV lithography. In *Extreme Ultraviolet (EUV) Lithography VIII*, volume 10143, page 1014308. International Society for Optics and Photonics, March 2017.

[116] Hyo-Jun Kim, Min-Ho Shin, Hyun-Guk Hong, Bo-Sun Song, Soo-Kang Kim, Won-Hoe Koo, Jong-Geun Yoon, Soo-Young Yoon, and Young-Joo Kim. Enhancement of Optical Efficiency in White OLED Display Using the Patterned Photoresist Film Dispersed with Quantum Dot Nanocrystals. *Journal of Display Technology*, 12(6):526–531, June 2016.

[117] Maxime Puyo, Pierre Fau, Myrtil L. Kahn, David Mesguich, Jérôme Launay, and Katia Fajerwerg. Removable Composite Electrode Made of Silver Nanoparticles on Pyrolyzed Photoresist Film for the Electroreduction of 4-Nitrophenol. *Langmuir*, September 2019.

[118] Kazuki Kasahara, Vasiliki Kosma, Jeremy Odent, Hong Xu, Mufei Yu, Emmanuel P. Giannelis, and Christopher K. Ober. Recent progress in nanoparticle photoresists development for EUV lithography. In *Extreme Ultraviolet (EUV) Lithography VII*, volume 9776, page 977604. International Society for Optics and Photonics, March 2016.

[119] Richard A. Lawson and Alex P. G. Robinson. Chapter 1 - Overview of materials and processes for lithography. In Alex Robinson and Richard Lawson, editors, *Frontiers of Nanoscience*, volume 11 of *Materials and Processes for Next Generation Lithography*, pages 1–90. Elsevier, January 2016.

[120] L. Bissi, M. Cicioni, P. Placidi, S. Zampolli, I. Elmi, and A. Scorzoni. A Programmable Interface Circuit for an Ultralow Power Gas Sensor. *IEEE Transactions on Instrumentation and Measurement*, 60(1):282–289, January 2011.

[121] S. Bagga, N. Bhat, and S. Mohan. LPG Gas-Sensing System with Thin-Film Transducer and CMOS Signal Conditioning ASIC. *IEEE Transactions on Instrumentation and Measurement*, 58(10):3653–3658, October 2009.

[122] A. Ponzoni, A. Depari, E. Comini, G. Faglia, A. Flammini, and G. Sberveglieri. Exploitation of a low-cost electronic system, designed for low-conductance and wide-range measurements, to control metal oxide gas sensors with temperature profile protocols. *Sensors and Actuators B: Chemical*, 175:149–156, December 2012.

[123] X. Mu, D. Rairigh, and A. J. Mason. 125ppm resolution and 120dB dynamic range nanoparticle chemiresistor array readout circuit. In *2011 IEEE International Symposium of Circuits and Systems (ISCAS)*, pages 2213–2216, May 2011.

[124] H. Y. Seong, S. Kweon, J. Suh, J. Lee, C. Park, Y. Jung, and M. Je. Technical Review: Interface Integrated Circuits for Metal-Oxide Gas Sensors. In *2018 IEEE International Conference on Consumer Electronics - Asia (ICCE-Asia)*, pages 206–212, June 2018.

[125] C. K. Leung and D. M. Wilson. Integrated interface circuits for chemiresistor arrays. In *2005 IEEE International Symposium on Circuits and Systems*, pages 5914–5917 Vol. 6, May 2005.

[126] Harold V. Shurmer and Julian W. Gardner. Odour discrimination with an electronic nose. *Sensors and Actuators B: Chemical*, 8(1):1–11, April 1992.

[127] J. W. Gardner, P. K. Guha, F. Udrea, and J. A. Covington. CMOS Interfacing for Integrated Gas Sensors: A Review. *IEEE Sensors Journal*, 10(12):1833–1848, December 2010.

[128] Arkadiy Morgenshtein, Liby Sudakov-Boreysha, Uri Dinnar, Claudio G. Jakobson, and Yael Nemirovsky. Wheatstone-Bridge readout interface for ISFET/REFET applications. *Sensors and Actuators B: Chemical*, 98(1):18–27, March 2004.

[129] J. W. Gardner, M. Vidic, P. Ingleby, A. C. Pike, J. E. Brignell, P. Scivier, P. N. Bartlett, A. J. Duke, and J. M. Elliott. Response of a poly(pyrrole) resistive micro-bridge to ethanol vapour. *Sensors and Actuators B: Chemical*, 48(1):289–295, May 1998.

[130] M Cole, J. W Gardner, A. W. Y Lim, P. K Scivier, and J. E Brignell. Polymeric resistive bridge gas sensor array driven by a standard cell CMOS current drive chip. *Sensors and Actuators B: Chemical*, 58(1):518–525, September 1999.

[131] Svante Wold, Kim Esbensen, and Paul Geladi. Principal component analysis. *Chemometrics and Intelligent Laboratory Systems*, 2(1-3):37–52, August 1987.

[132] Changsong Wang, Chaofu Ke, Xiaoyang Wang, Chunjie Chi, Lei Guo, Suqi Luo, Zhigang Guo, Guowang Xu, Fengmin Zhang, and Enyou Li. Noninvasive detection of colorectal cancer by analysis of exhaled breath. *Analytical and Bioanalytical Chemistry*, 406(19):4757–4763, July 2014.

[133] M. Hakim, S. Billan, U. Tisch, G. Peng, I. Dvrokind, O. Marom, R. Abdah-Bortnyak, A. Kuten, and H. Haick. Diagnosis of head-and-neck cancer from exhaled breath. *British Journal of Cancer*, 104(10):1649–1655, May 2011.

[134] Annette G. Dent, Tom G. Sutedja, and Paul V. Zimmerman. Exhaled breath analysis for lung cancer. *Journal of Thoracic Disease*, 5(Suppl 5):S540–S550, October 2013.

[135] Yanyue Yan, Qihui Wang, Wenwen Li, Zhongjun Zhao, Xin Yuan, Yanping Huang, and Yixiang Duan. Discovery of potential biomarkers in exhaled breath for diagnosis of type 2 diabetes mellitus based on GC-MS with metabolomics. *RSC Advances*, 4(48):25430–25439, June 2014.

[136] Gang Peng, Ulrike Tisch, Orna Adams, Meggie Hakim, Nisrean Shehada, Yoav Y. Broza, Salem Billan, Roxolyana Abdah-Bortnyak, Abraham Kuten, and Hossam Haick. Diagnosing lung cancer in exhaled breath using gold nanoparticles. *Nature Nanotechnology*, 4(10):669–673, October 2009.

[137] M. Aleixandre, J. Lozano, J. Gutiérrez, I. Sayago, M. J. Fernández, and M. C. Horrillo. Portable e-nose to classify different kinds of wine. *Sensors and Actuators B: Chemical*, 131(1):71–76, April 2008.

[138] Min Xu, Jun Wang, and Shuang Gu. Rapid identification of tea quality by E-nose and computer vision combining with a synergetic data fusion strategy. *Journal of Food Engineering*, 241:10–17, January 2019.

[139] Yong Yin and Yuzhen Zhao. A feature selection strategy of E-nose data based on PCA coupled with Wilks -statistic for discrimination of vinegar samples. *Journal of Food Measurement and Characterization*, 13(3):2406–2416, September 2019.

[140] Ian T. Jolliffe and Jorge Cadima. Principal component analysis: a review and recent developments. *Philosophical Transactions of the Royal Society A: Mathematical, Physical and Engineering Sciences*, 374(2065):20150202, April 2016.

[141] Alaa Tharwat, Tarek Gaber, Abdelhameed Ibrahim, and Aboul Ella Hassanien. Linear discriminant analysis: A detailed tutorial. *AI Communications*, 30(2):169–190, January 2017.

[142] Federica Bianchi, Nicolò Riboni, Paolo Carbognani, Letizia Gnetti, Enrico Dalcanale, Luca Ampollini, and Maria Careri. Solid-phase microextraction coupled to gas chromatography–mass spectrometry followed by multivariate data analysis for the identification of volatile organic compounds as possible biomarkers in lung cancer tissues. *Journal of Pharmaceutical and Biomedical Analysis*, 146:329–333, November 2017.

[143] D'Nisha Hamblin and José Almirall. Analysis of exhaled breath from cigarette smokers using CMV-GC/MS. *Forensic Chemistry*, 4:67–74, June 2017.

[144] Gustavo Yasuo Figueiredo Makimori and Evandro Bona. Commercial Instant Coffee Classification Using an Electronic Nose in Tandem with the ComDim-LDA Approach. *Food Analytical Methods*, 12(5):1067–1076, May 2019.

[145] Xue-Mei Jia, Qing-Hao Meng, Ya-Qi Jing, Pei-Feng Qi, Ming Zeng, and Shu-Gen Ma. A New Method Combining KECA-LDA With ELM for Classification of Chinese Liquors Using Electronic Nose. *IEEE Sensors Journal*, 16(22):8010–8017, November 2016.

[146] Markus R. Meyer, Frank T. Peters, and Hans H. Maurer. Automated mass spectral deconvolution and identification system for GC-MS screening for drugs, poisons, and metabolites in urine. *Clinical chemistry*, 56(4):575–584, 2010.

[147] Mark P. Styczynski, Joel F. Moxley, Lily V. Tong, Jason L. Walther, Kyle L. Jensen, and Gregory N. Stephanopoulos. Systematic identification of conserved metabolites in GC/MS data for metabolomics and biomarker discovery. *Analytical chemistry*, 79(3):966–973, 2007.

[148] Ali Daneshkhah. Statistical Analysis to Identify Volatile Organic Compounds (VOCs) in Breath from Hypoglycemia and Development of Cross-Selective Nanosensors for its Detection. *Theses and Dissertations Available from ProQuest*, pages 1–142, January 2017.

[149] Li Han, Xiajing Shi, Wendy Wu, F. Louis Kirk, Jin Luo, Lingyan Wang, Derrick Mott, Lisa Cousineau, Stephanie I-Im Lim, Susan Lu, and Chuan-Jian Zhong. Nanoparticle-structured sensing array materials and pattern recognition for VOC detection. *Sensors and Actuators B: Chemical*, 106(1):431–441, April 2005.

[150] Amir Zabet-Khosousi and Al-Amin Dhirani. Charge Transport in Nanoparticle Assemblies. *Chemical Reviews*, 108(10):4072–4124, October 2008.

[151] James Scott Cooper, Burkhard Raguse, Edith Chow, Lee Hubble, Karl-Heinz Müller, and Lech Wieczorek. Gold Nanoparticle Chemiresistor Sensor Array that Differentiates between Hydrocarbon Fuels Dissolved in Artificial Seawater. *Analytical Chemistry*, 82(9):3788–3795, May 2010.

[152] Niti Garg, Ashok Mohanty, Nathan Lazarus, Lawrence Schultz, Tony R. Rozzi, Suresh Santhanam, Lee Weiss, Jay L. Snyder, Gary K. Fedder, and Rongchao Jin. Robust gold nanoparticles stabilized by trithiol for application in chemiresistive sensors. *Nanotechnology*, 21(40):405501, September 2010.

[153] *Dual 4-Channel Analog Multiplexer/Demultiplexer datasheet*, 2019 (accessed November 5, 2019). https://assets.nexperia.com/documents/datasheet/74HC$_H$*CT*4052*.pdf*.

[154] Bluno nano sku dfr0296-DFRobot, 2019 (accessed November 11, 2019). https://wiki.dfrobot.com/Bluno_Nano_SKU_DFR0296.

[155] *Arduino Integrated Development Environment (IDE)[Computer Software](2019)*. Retrived from https://www.arduino.cc/en/main/software.

[156] University of South Florida and Sanim Rahman. Size and Concentration Analysis of Gold Nanoparticles with Ultraviolet-Visible Spectroscopy. *Undergraduate Journal of Mathematical Modeling: One + Two*, 7(1), October 2016.